doi: 10.1111/j.1460-2695.2005.00878.x

Invited Article

A fracture mechanics and mechanistic approach to the failure of cortical bone

R. O. RITCHIE[1], J. H. KINNEY[2], J. J. KRUZIC[1,3] and R. K. NALLA[1]

[1]Materials Sciences Division, Lawrence Berkeley National Laboratory, and Department of Materials Science and Engineering, University of California, Berkeley, CA 94720, [2]Lawrence Livermore National Laboratory, Livermore, CA 94550, and [3]Department of Mechanical Engineering, Oregon State University, Corvallis, OR 97331, USA

Received in final form 28 October 2004

ABSTRACT The fracture of bone is a health concern of increasing significance as the population ages. It is therefore of importance to understand the mechanics and mechanisms of how bone fails, both from a perspective of outright (catastrophic) fracture and from delayed/time-dependent (subcritical) cracking. To address this need, there have been many *in vitro* studies to date that have attempted to evaluate the relevant fracture and fatigue properties of human cortical bone; despite these efforts, however, a complete understanding of the *mechanistic* aspects of bone failure, which spans macroscopic to nanoscale dimensions, is still lacking. This paper seeks to provide an overview of the current state of knowledge of the fracture and fatigue of cortical bone, and to address these issues, whenever possible, in the context of the hierarchical structure of bone. One objective is thus to provide a mechanistic interpretation of how cortical bone fails. A second objective is to develop a framework by which fracture and fatigue results in bone can be presented. While most studies on bone fracture have relied on linear-elastic fracture mechanics to determine a single-value fracture toughness (e.g., K_c or G_c), more recently, it has become apparent that, as with many composites or toughened ceramics, the toughness of bone is best described in terms of a resistance-curve (R-curve), where the toughness is evaluated with increasing crack extension. Through the use of the R-curve, the intrinsic and extrinsic factors affecting its toughness are separately addressed, where 'intrinsic' refers to the damage processes that are associated with crack growth ahead of the tip, and 'extrinsic' refers to the shielding mechanisms that primarily act in the crack wake. Furthermore, fatigue failure in bone is presented from both a classical fatigue life (S/N) and fatigue-crack propagation (da/dN) perspective, the latter providing for an easier interpretation of fatigue micromechanisms. Finally, factors, such as age, species, orientation, and location, are discussed in terms of their effect on fracture and fatigue behaviour and the associated mechanisms of bone failure.

Keywords bone; crack bridging; fatigue; fracture; microcracking; toughening.

NOMENCLATURE

A = scaling constant in the power law for sustained-load crack growth
a = crack length/flaw size
a_o and a_c = initial and final crack sizes, respectively
B = specimen thickness
C = specimen compliance
C' = scaling constant in the Paris law for fatigue-crack growth
da, Δa = crack growth/extension

Correspondence: R. O. Ritchie. E-mail: roritchie@lbl.gov

da/dN = crack-growth rate (with respect to fatigue cycles)
da/dt = crack velocity or crack-growth rate (with respect to time)
E = Young's modulus
f = cyclic (fatigue) frequency
G = strain-energy release rate
G_c = critical strain-energy release rate
G_I, G_{II} and G_{III} = mode I, II and III strain-energy release rates, respectively
K = stress-intensity factor
K_{app} = applied far-field stress intensity
K_{br} = bridging stress intensity
K_c = critical stress intensity
K_{max} and K_{min} = maximum and minimum stress intensity
K_o = crack-initiation toughness
K_{tip} = local stress intensity experienced at the crack tip
K_I, K_{II} and K_{III} = mode I, II and III stress intensities, respectively
ΔK = stress-intensity range ($= K_{max}–K_{min}$)
k_1 and k_2 = local mode-I and mode-II stress intensities, respectively
m = Paris law exponent for fatigue-crack growth
N = number of fatigue cycles
n = exponent for sustained-load crack growth
Q = dimensionless geometry factor in K solutions
R = load ratio (minimum load/maximum load) in fatigue
W_f = work of fracture
ν = Poisson's ratio
μ' = shear modulus
σ_Y = yield stress

INTRODUCTION

The structural integrity of mineralized tissues such as cortical bone is of great clinical importance, especially since bone forms the protective load-bearing skeletal framework of the body. Bone is unique when compared to structural engineering materials due to its well-known capacity for self-repair and adaptation to changes in mechanical usage patterns.[1–5] Unfortunately, ageing-related changes to the musculoskeletal system are known to increase the susceptibility of bone fracture.[6] In the case of the very elderly, such changes are a critical issue as the consequent fractures can lead to significant mortality.[7] While a number of extraosseous variables, such as loading regimen, incidence of traumatic falls, prior fractures, etc., are involved, it is well known that the primary factor is that bone tissue itself deteriorates with age.[8] A primary factor in bone tissue deterioration is "bone quality", where quality is a term used to describe some, but as yet clearly not known characteristics of the tissue that influence a broad spectrum of mechanical properties such as elastic modulus, strength and toughness. Traditional thinking concerning such bone quality and how it degrades with age has focused on the question of bone mass or bone mineral density (BMD, defined as the amount of bone mineral per unit cross-sectional area) as a predictor of such fracture risk. For example, the elevation in bone turnover, concurrent with menopause in ageing women, can lead to osteoporosis, a condition of low bone mass associated with an increased risk of fracture. The magnitude of the health problem that this entails is recognized from disease statistics from the National Osteoporosis Foundation (Washington, D.C.); one in two women and one in four men over the age of 50 will have an osteoporosis-related fracture in the course of their remaining lifetime. Though bone mass can explain some of the fracture risk, there is now mounting evidence that low BMD alone can not be the sole factor responsible for the ageing-induced fracture risk.[6,9,10] For example, the work by Hui *et al.*[6] showed a roughly 10-fold increase in fracture risk with ageing, independent of BMD. This result and the concurrent realization that bone mineral density alone cannot explain the therapeutic benefits of anti-resorptive agents in treating osteoporosis[10,11] has re-emphasized the necessity for understanding how other factors control bone quality and specifically bone fracture.

While most clinical fractures are a result of a single (traumatic) overload or dynamic fracture event, often in association with deteriorated (e.g. age-related) bone quality, there is also clinical significance for fractures that occur over time; these are referred to as so called 'stress fractures', and result from subcritical crack growth caused by periods of sustained and/or cyclic loading.[5,12–14] Stress fractures are a well-recognized clinical problem with per

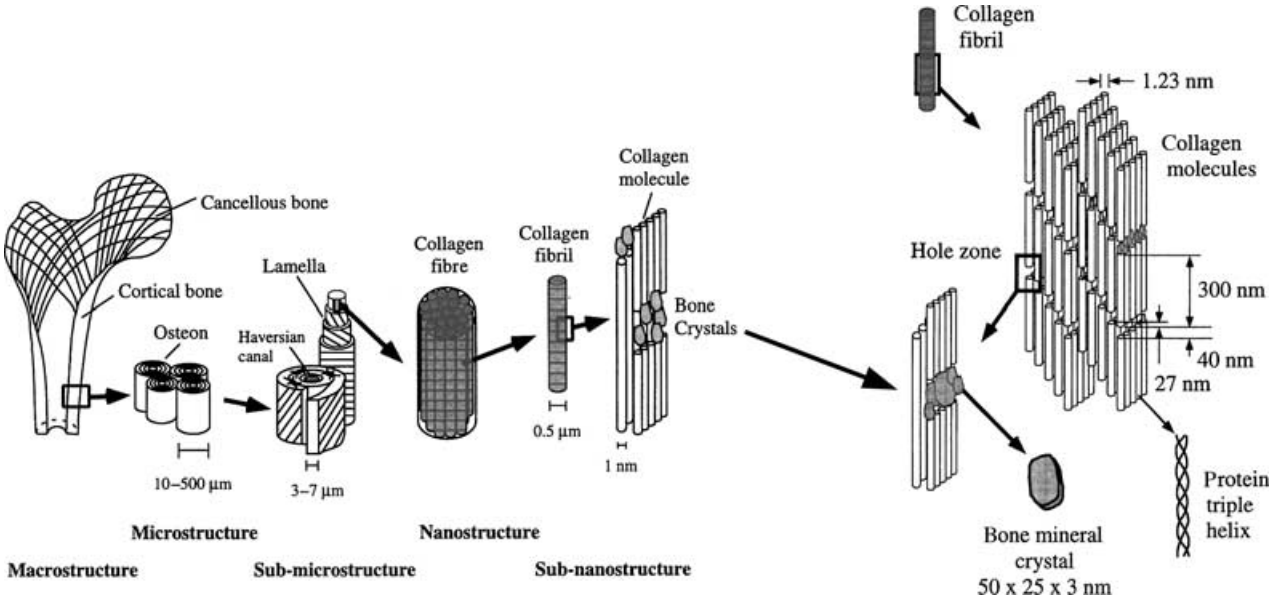

Fig. 1 The hierarchical microstructure of human cortical bone, showing the osteons with the Haversian canals that are the most recognizable feature. The structure of collagen with the regular 67 nm spacing (40 nm hole zone and 27 nm overlap zone) is also shown. Figure reproduced from Rho *et al.*[16]

capita incidences of 1–4% often being reported,[5,13] with even higher rates cited for adolescent athletes and military recruits.[5,12,14] They are commonly seen within a few weeks of a sudden systematic increase in the loading levels experienced by the bone, when the time elapsed is insufficient for an adaptational response to alleviate the deleterious effects of the increased stress levels.[5] In addition, cyclic loading may be a factor in so-called 'fragility' fractures commonly seen in the elderly, where there is increased fracture risk due to reduced bone quality.[5] In this review, we examine the differing modes of cortical bone failure and consider how the mechanisms of fracture relate to the structure of bone, defined broadly from 'micro' to 'nano' size scales.

The microstructure of cortical bone is hierarchical and is, indeed, quite complex. The basic building blocks, an organic matrix (roughly 90% type-I collagen, 10% other organic materials, mainly proteins) and mineral phase (calcium phosphate-based apatite mineral), are similar for all collagen-based mineralized tissues, although the ratio of these components and the complexity of the hydrated structures that they form vary with the function of the particular tissue and the organ it forms. In addition to the hierarchical complexity, the composition and the structure of bone vary with factors such as skeletal site, age, sex, physiological function and mechanical loading, making bone a very heterogeneous structure, with the need for vascularization adding to the complexity of the tissue. On average, though, the organic/mineral ratio in human cortical bone is roughly 1:1 by volume and 1:3 by weight.[15]

The hierarchical structure of cortical bone (Fig. 1) can be considered at several dimensional scales.[16–18] At nanoscale dimensions, bone is composed of type-I mineralized collagen fibres (up to 15 μm in length, 50–70 nm in diameter and bundled together) made up of a regular, staggered arrangement of collagen molecules.[16] These fibres are bound and impregnated with carbonated apatite nanocrystals (tens of nm in length and width, 2–3 nm in thickness),[16] and are further organized at microstructural length-scales into a lamellar structure with adjacent lamellae being 3–7 μm thick.[17] Generally oriented along the long axis of bones are the secondary osteons[18] (up to 200–300 μm diameter), composed of large vascular channels (up to 50–90 μm diameter) surrounded by circumferential lamellar rings, with so-called 'cement lines' at the outer boundary. The aetiology of the secondary osteons lies in the remodelling process that is used to repair damage *in vivo*.

For developing a realistic understanding of how factors such as age, species, orientation, or location affect the fracture resistance of bone, it is critical to assess the importance of the various microstructural features in determining the mechanical properties. In short, the difficulty lies in determining the roles that the underlying microstructural constituents, including their properties and their morphological arrangement, play in crack initiation, subsequent crack propagation and final unstable fracture and in separating these effects. This present work intends to describe how fracture mechanics, along with various characterization techniques, have been used to begin the

development of such a mechanistic framework for the failure behaviour of cortical bone. This paper considers the large body of literature that address these issues through 'single-value' fracture toughness measurements such as the work of fracture, W_f, the critical stress-intensity factor, K_c, or the critical strain-energy release rate, G_c, before discussing more recent results that demonstrate that cracking in bone involves *rising* fracture resistance with crack extension. Additionally, the role of fatigue, by repetitive cyclic loading or sustained static loading, on cortical bone failure will be reviewed. In all cases, the failure behaviour of bone will be discussed, when possible, in light of the salient fracture and fatigue mechanisms involved.

FRACTURE TOUGHNESS BEHAVIOUR

K_{Ic} and G_{Ic} fracture toughness measurements

The work of fracture method is one approach which has been used to characterize the toughness of cortical bone.[19–24] For this technique the area under the load–displacement curve measured during the failure of a nominally 'flaw free' specimen is divided by twice the nominal crack-surface area to obtain the work of fracture, W_f. A major drawback of this method, however, is that results can be both size- and geometry-dependent. Thus, while W_f may be used successfully to assess trends when the nominal sample size and geometry are held constant, such results are not generally useful for comparing values determined in different studies, which employed different sample geometries.

Accordingly, the fracture properties of cortical bone may be better characterized by utilizing linear-elastic fracture mechanics. In this case, for an essentially linear-elastic material, where any inelastic (e.g., yielding) behaviour is limited to a small near-tip region, the stress and displacement fields local to the tip of a pre-existing crack are described by the stress-intensity factor, K. The stress-intensity factor may be defined for mode I (tensile-opening loading), mode II (shear loading) or mode III (tearing or anti-plane shear loading) in terms of the geometrical crack configuration, applied stress, σ_{app}, and crack size, a, viz:[25]

$$K_{(I,II,III)} = Q\sigma_{app}(\pi a)^{1/2}, \tag{1}$$

where Q is a dimensionless constant dependant on sample geometry and loading mode (i.e. mode I, II or III) (Fig. 2). The resistance to fracture, or fracture toughness, is then defined for particular mode of loading as the critical value of the stress intensity, K_c, at the onset of unstable fracture, as usually computed from the peak stress.

Alternatively, many investigations of the fracture resistance of bone have expressed toughness in terms of a critical value of the strain-energy release rate, G_c, defined as the change in potential energy per unit increase in crack area at fracture; this may be expressed as:[25]

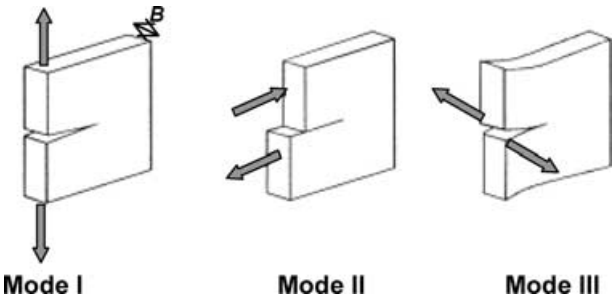

Fig. 2 Schematic illustrating the different modes of loading: mode I (tensile-opening loading), mode II (shear loading) and mode III (tearing or anti-plane shear loading). Loading *in vivo* could involve one or more of these modes.

$$G_c = \frac{P^2}{2B}\frac{dC}{da}, \tag{2}$$

where P is the applied load, B the specimen thickness and dC/da is the change in sample compliance with crack extension (the compliance, C, is the slope of the displacement–load curve). It is important to note that for linear-elastic materials, G and K, are uniquely related via:

$$G = \frac{K_I^2}{E'} + \frac{K_{II}^2}{E'} + \frac{K_{III}^2}{2\mu'}, \tag{3}$$

where E' is the appropriate elastic modulus ($E' = E$ in plane stress, $E/(1-\nu^2)$ in plane strain, where E is Young's modulus and ν is Poisson's ratio) and μ' is the shear modulus.[25] If linear-elastic conditions prevail, that is, inelastic deformation is limited to a small zone near the crack tip, both G_c and K_c should give a geometry-independent measure of toughness, provided plane-strain conditions are met, as described below. Some typical mode I fracture toughness values measured for bone, tabulated from various sources, are summarized in Table 1; definitions for the orientations used in those tests may be seen in Fig. 3. Table 2 gives single-value toughness in terms of K and G for cortical bone, as compared to some common structural materials. It is interesting to note that when the toughness is assessed in terms of K, bone and dentin (a mineralized tissue which makes up the bulk of the human tooth and is very similar to bone at the nanostructural level) have toughness values similar to common engineering ceramics, such as silicon carbide. However, when assessed in terms of G, bone is some one to two orders of magnitude tougher owing to its much lower Young's modulus (see Table 2).

Effect of loading mode

Cortical bone shows the least resistance to fracture under mode I (purely tensile) loading, and accordingly this loading mode has received the most attention in the

Table 1 Examples of mode-I single-value fracture toughness results for cortical bone using compact tension, C(T), and single-edge-notched bend, SEN(B), specimens taken from various sources

Species	Bone	Orientation[a]	K_c (MPa$\sqrt{m}$)	G_c (J/m^2)	Test geometry	References
Bovine	Femur	Long	3.6 ± 0.7		C(T)	32
Bovine	Femur	Long	2.4–5.2[b]	920–2780[b]	C(T)	115
Bovine	Femur	Transverse	5.7 ± 1.4		SEN(B)	133
Bovine	Femur	L-R	3.4–5.1[e]		SEN(B)	20
Bovine	Femur	C-L	2.1–2.9[e]		SEN(B)	20
Bovine	Tibia	Long	4.5–5.4[b]	760–2130[b]	C(T)	116
Bovine	Tibia	Long	2.8–6.3[b]	630–2880[b]	C(T)	33
Bovine	Tibia	Long	3.2		C(T)	35
Bovine	Tibia	Transverse	6.4		C(T)	35
Bovine	Tibia	L-R	4.5–6.6[e]		SEN(B)	20
Baboon	Femur	Long	1.8 ± 0.5		C(T)	36
Baboon	Femur	Transverse	6.2 ± 0.7		SEN(B)	36
Baboon	Femur	Long	1.7–2.3[d]		C(T)	55
Human	Femur	L-C	6.4 ± 0.3		SEN(B)	24
Human	Femur	C-L		520 ± 190	C(T)	38
Human	Tibia	C-L		400 ± 250	C(T)	38
Human	Tibia	C-L	4.1–4.3[c]	600–830[c]	C(T)	34
Human	Humerus	C-R	2.2 ± 0.2		SEN(B)	37
Human	Humerus	C-L	3.5 ± 0.1		SEN(B)	37
Human	Humerus	L-C	5.3 ± 0.4		SEN(B)	37
Human	Femur	Transverse	4.3–5.4[d]		SEN(B)	19

Data are given in either K or G as reported by the authors. All reported values are mean values, standard deviations are given when possible.
[a]When specific orientation is unknown, cracking direction is given, see Fig. 3 for details.
[b]Range of mean values for several sets of data from samples tested at different loading rates.
[c]Range of mean values for two sets of data using samples of different thickness.
[d]Range of mean values for three sets of data using samples from different age groups.
[e]Range of mean values for two sets of data using samples stored in different media.

literature. For example, in human tibiae[26] and femurs,[27] average ratios of G_{IIc}/G_{Ic} of 12.7 and 4.6, respectively, have been measured for longitudinal (C-L) fracture and donors aged between 50 and 90 years. Similarly, higher mode II G_{IIc} values relative to G_{Ic} have been reported for human femoral neck.[28] Using bovine femora, a recent study focused on mode I, II and III fracture and found G_{IIc}/G_{Ic} and G_{IIIc}/G_{Ic} to be 3.8 and 2.6, respectively, for longitudinal fracture and 3.4 and 2.9, respectively, for transverse fracture.[29] Although such results suggest mode III fracture may be easier than mode II, it is unclear whether this will be true for all species, locations, orientations and other variables. Because it is invariably 'worst-case', is the most common failure mode and has received the most attention in the literature, mode I fracture will be the subject of the remainder of this article.

Plane stress versus plane strain

In applying fracture mechanics to most materials, if the sample has a thickness significantly larger than the scale of local inelasticity, K_c or G_c values should be thickness-, geometry- and crack-size independent and a condition of plane strain is said to exist. However, with thinner specimens, the toughness values may be significantly higher and not independent of such factors as conditions approach those of plane stress. The ASTM standard for mode I fracture toughness testing of metals, that is, ASTM E-399, requires that[30]

$$B \geq 2.5 \left(\frac{K_I}{\sigma_Y} \right)^2, \tag{4}$$

for plane-strain conditions to exist, where B is the specimen thickness and σ_Y is the yield stress of the material. Because of variations in K_I and σ_Y with factors such as species, location and orientation, the condition in Eq. 4 may not always be strictly met for fracture testing of cortical bone, particularly for human bone, which is of the most clinical interest. For example, based on properties compiled in Ref. [31], a thickness ranging from ~1 to 10 mm may be required to meet plane-strain conditions in human cortical bone, depending upon location, age and orientation, demonstrating how Eq. 4 may not always be easily satisfied for all practical testing. It should be noted, however, that Eq. 4 is typically considered conservative for most engineering materials and its specific relevance to cortical bone has not been thoroughly explored. In an

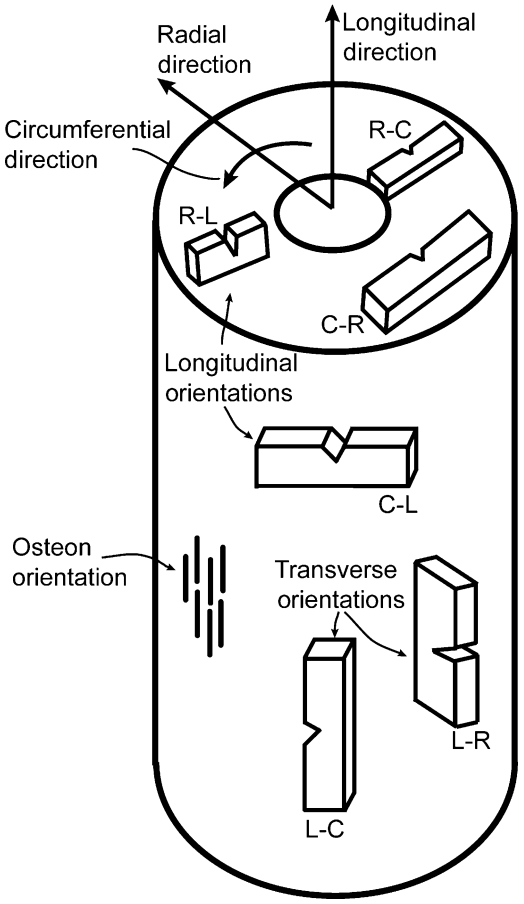

Fig. 3 Schematic illustrating the orientation code used by the ASTM E399 fracture toughness standard.[30] The first letter in the designation refers to the normal direction to the crack plane, while the second letter refers to the expected direction of crack propagation. It is seen that the L-C and L-R orientations involve transversely cutting the osteons, and accordingly these orientations are commonly referred to as having a transverse cracking direction in the literature. Conversely, orientations which split apart the osteons along the longitudinal axis (R-L and C-L) are commonly referred to as orientations with longitudinal cracking. Often the specific transverse or longitudinal orientation is not given, however, the L-C and C-L orientations are the easiest to machine, especially from smaller bones. Finally, the orientations splitting the osteons along their short axes (C-R and R-C) are the least common orientations found in the fracture literature.

early study, no thickness dependence was found for mode I longitudinal cracking (see Fig. 3 for details on orientation designation) in bovine femora for 1.8–3.8 mm thick specimens;[32] a similar conclusion was reached for mode I fracture of bovine tibia, also in the longitudinal direction, where no thickness dependence was seen between 0.5 and 2 mm.[33] Conversely, more recent studies by Norman *et al.* report that the mode I toughness varied significantly with thickness from 2 to 6 mm, becoming essentially constant after a thickness of 6 mm was achieved.[34] Limited experiments on human tibia also showed little change in mode I toughness for 2 to 3 mm thick specimens.[34] Thus, until more extensive information on this subject is available, caution should be used when comparing fracture data on bone from different studies which used appreciably different specimen thicknesses.

Table 2 Typical range of (mode I) single-value fracture toughness values given in both K and G for cortical bone in comparison to dentin another mineralized tissue and a number of common engineering materials

Material	E (GPa)	K_c (MPa$\sqrt{m}$)	G_c (kJ/m^2)
Cortical bone	15–25	2–7	0.15–3.25
Dentin	20–25	1–2	0.05–0.2
Titanium alloy (Ti–6Al–4V)	110	65–100	40–90
High strength steel (4340)	210	50–100	10–45
Commercial silicon carbide	400	3	0.02
Silicon	110	1	0.01

Effect of microstructural orientation and anatomical location

The orientation relationship between the crack and the bone has a profound influence on the fracture resistance of cortical bone tissue (Fig. 4a). Specifically, transverse cracking directions (L-C and L-R), that is, where the crack must cut the osteons, have been found to be consistently tougher than orientations with longitudinal cracking (C-L and R-L), where the crack splits osteons along the longitudinal axis of the bone. In bovine tibia, Behiri and Bonfield demonstrated a progressive increase in toughness (from 3.2 to 6.5 MPa$\sqrt{m}$) as the orientation of specimens was varied rotationally from the longitudinal to transverse cracking directions.[35] In order to achieve straight crack propagation in all but the longitudinal orientation, side grooving of specimens was required, otherwise cracks would kink towards the longitudinal direction, as shown in Fig. 4c for human bone. Many studies have confirmed this behaviour; indeed, K_{Ic} for transverse cracking was found to be up to twice that for longitudinal cracking in bovine tibia[20,35] and femora.[20,29] Furthermore, a study on baboon femora showed an even larger effect, with a mean K_{Ic} for fracture in the transverse direction some 3.5 times higher than in the longitudinal direction.[36] Finally, in human humeri, similar behaviour has been observed, with cracks kinking ~90° towards the longitudinal direction (anatomically proximal-distal) when cracking in the transverse direction was attempted (Fig. 4c), with transverse toughness (L-C) reported to be 1.5 times the longitudinal (C-L) (5.3 vs. 3.5 MPa$\sqrt{m}$); conversely, the C-R orientation, which splits the osteons along the short axis, showed the lowest toughness of 2.2 MPa$\sqrt{m}$ (Fig. 4a).[37] It should be noted that the latter two studies did not use specimen side grooving to ensure cracking in the

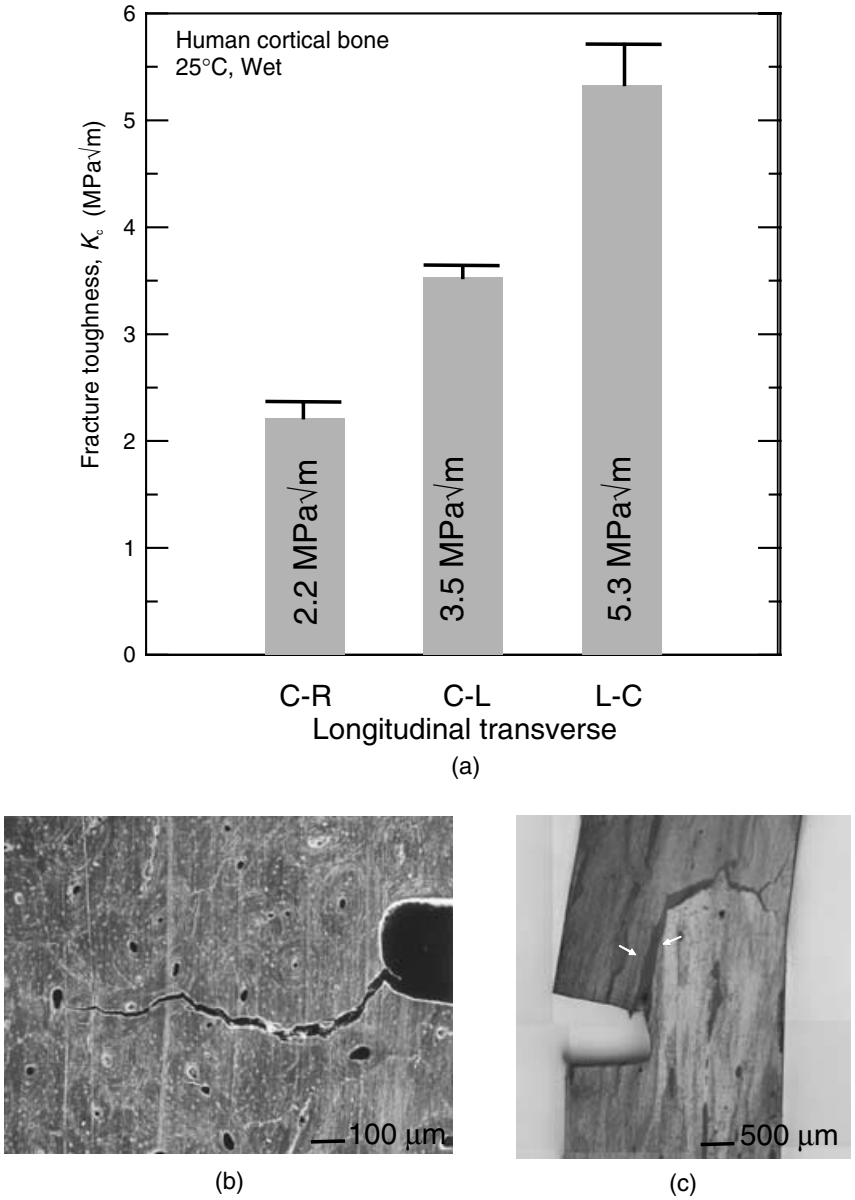

Fig. 4 (a) Variation in fracture toughness with orientation in human humeral cortical bone. Note the significantly higher toughness for the transverse (circumferential) orientation. The toughness in the transverse (L-C) case was ascribed to deflection of the crack due to the strong role of the cement line in that orientation (Courtesy: Nalla *et al.*[84]). Micrographs illustrating typical crack paths in the (b) C-R (SEM image), and (c) L-C (optical image) orientations. Note the ~90° crack deflection (indicated by white arrows) for the L-C oriented specimen into the longitudinal direction along a cement line in human cortical bone taken from the humerus.

transverse directions, and accordingly the transverse toughness values may be lower-bounds, that is, the orientation effect may be even larger than was reported in those studies. Some fracture toughness results for different orientations from studies in the archival literature may be found in Table 1.

Bone location is also thought to have an effect on fracture toughness; however, it is often difficult to separate other variables that might be involved to determine the significance of such differences. One study compared the toughness of femoral neck, femoral shaft, and tibial shaft specimens from matched human cadaveric bones in order to isolate the effect of bone location.[38] For identically sized C-L oriented specimens, the femoral shaft demonstrated significantly higher average G_{Ic} values relative to tibial shaft specimens (520 vs. 400 J/m^2). Although there were difficulties in comparing femoral neck data directly due to sample size restrictions, results suggested a significantly higher toughness than both the femoral and the tibial shaft specimens. Thus, it appears that bone location

does indeed have an effect on the toughness; however, it is not yet clear what microstructural differences associated with various locations may cause such toughness changes. Some toughness results for different anatomical locations within the same species are also included in Table 1.

Effects of microstructural factors

Many of the factors that influence the fracture of bone, such as age, location and orientation, are thought to be related to microstructural differences in the cortical bone tissue, either through changes in the morphology of the bone microstructure, or the properties of the constituents (e.g., collagen). For example, it has long been observed that changes in bone density and mineral content may be associated with changes in the toughness of bone. Studies on human and bovine bone have reported increases in toughness with increasing dry and wet density,[28,32,39] and decreases in toughness with increasing mineral content[22,23] or porosity.[40] While such results support the notion that bone fragility and osteoporosis may be associated with such factors, it does not fully explain, for example, sex differences in fracture rates.[41] Furthermore, there have also been studies that show the fracture toughness to be independent of bone density (BMD) or mineral content,[36,42,43] even when decreases in toughness with age were observed.[36,43]

More recently, excessive tissue repair/remodelling has been suggested as a possible cause for increasing fracture risk with age;[10,11] such remodelling can lead to loss in bone mass, but more importantly may also result in other morphological changes to the microstructure of bone. With regard to these microstructural factors, fractographic studies have suggested that both *in vivo* and *in vitro* fracture occurs more readily in human bone where there are fewer and smaller osteons.[44] In contrast, an *in vitro* fracture toughness study of longitudinal cracking in human femur and tibia specimens found higher toughness with smaller osteons and increasing osteonal density;[40] however, no significant relationships with these factors could be found for femoral neck cortical bone specimens,[28] which did not show a decrease in toughness with age.

The cement line, the boundary between secondary osteons and the surrounding lamellar matrix, is another microstructural element that, together with the collagen fibre orientation, is thought to play a key role in the fracture of bone. Indeed, both microcracks and macroscopic cracks have been observed to deflect (apparently) along the cement lines upon encountering osteons (Fig. 4c), leading to the conclusion that the cement line must provide a weak path for fracture.[37,45–49] Furthermore, the weak path provided by the cement lines may be responsible for the strong orientation effects seen in the fracture of bone, that is, the crack deflection of transverse cracks towards the longitudinal direction may be due to the cement lines, as suggested in Refs [36,37]. The exact nature of the cement line, however, is still not fully understood, and is clearly a topic worthy of further investigation.

Finally, changes in the mechanical properties of the microstructural constituents, principally collagen, may also have a significant effect on fracture resistance. Research into the effect on the fracture toughness of collagen denaturation, achieved both thermally and chemically,[21,50] found significant decreases in the work of fracture of human femur specimens with increasing amounts of denaturation. Another study on the effect of storage in alcohol *versus* saline[20] reported an elevation in toughness with storage in alcohol. It has been suggested that storage in a similar polar solvents (methanol and acetone) increases the collagen cross-link density via enhanced intermolecular hydrogen bonding in demineralized dentin;[51] it is conceivable that a similar phenomenon is responsible for the observations on bone in Ref. [20].

Effect of age

A critical issue with bone fracture is the problem of ageing. Indeed, a large number of studies that have looked at age-related issues in the mechanical properties of bone have implied a significant deterioration of the fracture toughness with age,[19,22–24,27,28,36,38,43,52–56] some results showing this trend may be seen in Fig. 5. In particular,

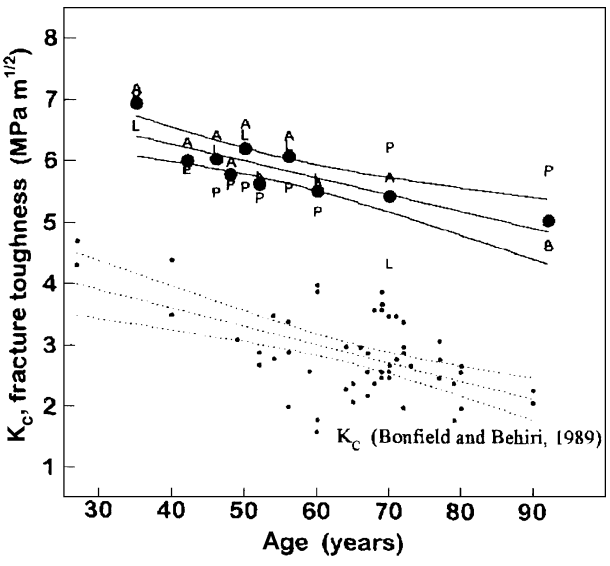

Fig. 5 Variation in fracture toughness with age in human cortical bone. Data for transverse (circumferential) (L-C) crack growth in femoral bone (top) and for longitudinal (C-L) crack growth in tibial bone (bottom) are included. Note the clear trend of decreasing toughness with age and that the effect of orientation is consistent with that previously discussed (Courtesy: Zioupos and Currey[24]).

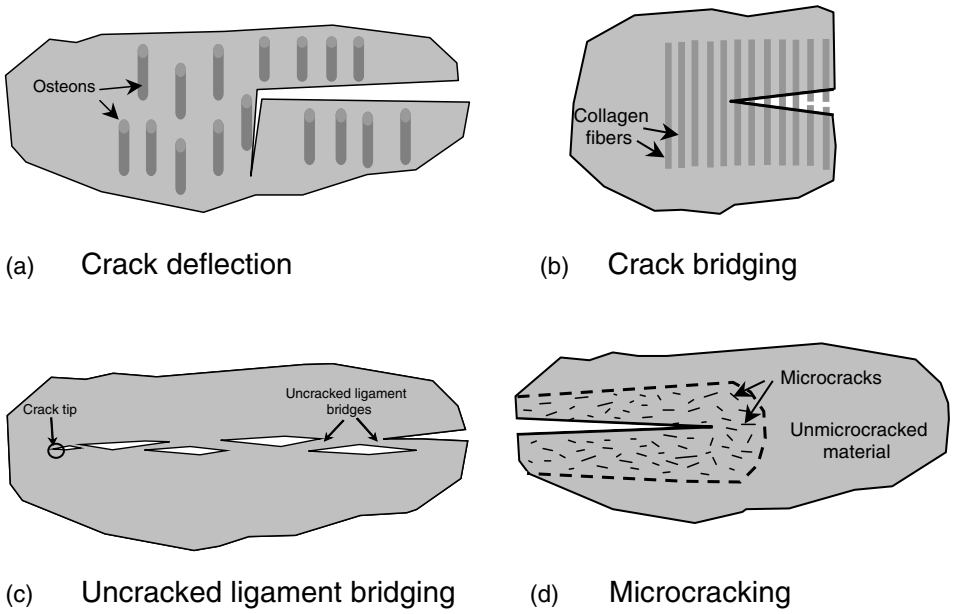

Fig. 6 Schematic illustrations of some of the toughening mechanisms possible in cortical bone. (a) Crack deflection (by osteons), (b) crack bridging (by collagen fibres), (c) uncracked-ligament bridging, and (d) diffuse microcracking. One or more of these mechanisms can be expected to be active.

ageing has been associated with changes in mineralization,[56–59] and lowered collagen network integrity,[19] with resultant reduction in the elastic deformability and toughness.[5,19,24,36,38,55,56] Also, it has been suggested that remodelling induced by increasing microdamage with ageing[4] leads to an increase in the difference in properties of the matrix (primary lamellar bone) and the secondary osteons, implying a stronger role for the cement lines and a reduction in the toughness.[5,24,36,47] Indeed, if specific age-related changes within the microstructure of bone can be linked to a reduced fracture resistance, progress can be made towards creating successful treatments to combat these deleterious effects.

Resistance-curve behaviour

In cases where specific extrinsic toughening mechanisms are active, such as in bone, the fracture resistance actually increases with crack extension, requiring a resistance-curve (R-curve) fracture-mechanics approach[25,60] to more accurately describe the fracture behaviour. This can be understood by appreciating that crack propagation is a mutual competition between two classes of mechanisms: *intrinsic* mechanisms, which are microstructural damage mechanisms that operate ahead of the crack tip, and *extrinsic* mechanisms, which act to 'shield' the crack from the applied driving force and operate principally behind the crack tip in the crack wake.[61–63] Rising R-curve behaviour is the direct result of extrinsic toughening mechanisms, which cause the crack-size dependence of the toughness.[61–63] Examples of such extrinsic mechanisms seen in engineering materials are crack bridging and constrained microcracking (Fig. 6). In such instances, crack extension commences at a *crack-initiation toughness*, K_o, while further crack extension requires higher driving forces until a 'plateau' or steady-state toughness is reached. The corresponding slope of the R-curve can be considered as a measure of the *crack-growth toughness*. While important for understanding the fracture behaviour of bone, R-curve analysis is also important for understanding, and differentiating, the intrinsic and extrinsic mechanisms involved in fracture.

Several recent studies[64–70] have revealed rising R-curve behaviour in bone (Fig. 7), indicative of the presence of active extrinsic toughening mechanisms in the crack wake. One of the first R-curve studies in bone, by Vashishth *et al.*[64] (Fig. 7a), looked at crack propagation in human and bovine tibia (human donor: 59 years old) for cracking in the longitudinal (proximal-distal) direction. It was found that the toughness of human and bovine bone specimens, respectively, rose linearly over the range of 1.6 to 2.5 MPa$\sqrt{}$m and 3.9 to 7.2 MPa$\sqrt{}$m for crack extensions of ~2.25 mm; initiation K_o values were found to be 1.6 and 3.9 MPa$\sqrt{}$m for human and bovine bone, respectively. A more recent study by Pezzoti and Sakakura[67] also reported a rising R-curve in bovine bone; however after an initial rising portion, a steady-state (so called 'plateau' toughness) was achieved, typical of many materials which exhibit R-curve behaviour (Fig. 7b). These authors gave values of ~3.2 MPa$\sqrt{}$m and ~5 MPa$\sqrt{}$m/mm for the

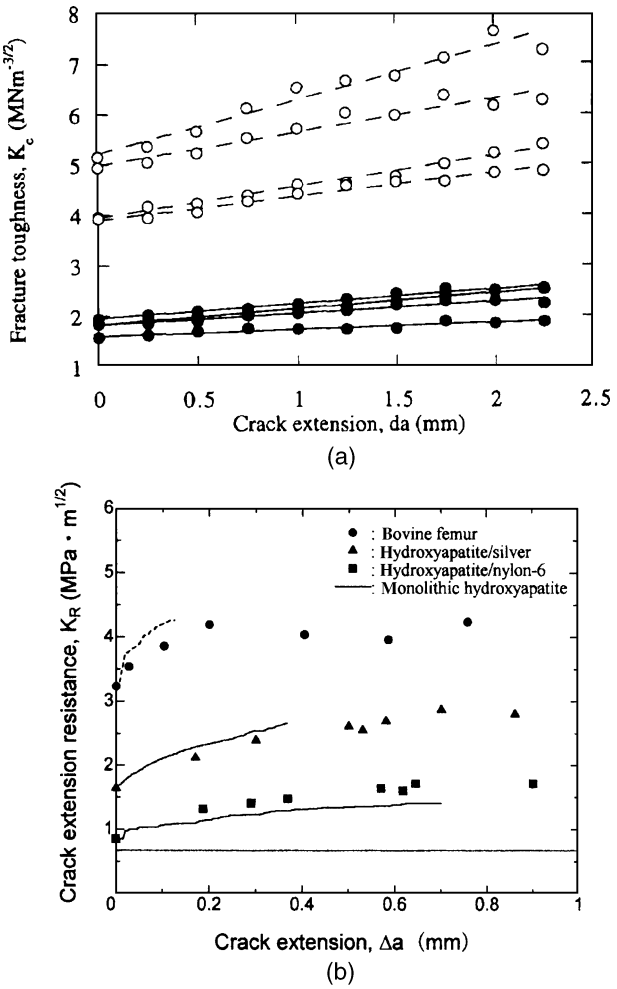

Fig. 7 Resistance-curve data for: (a) human (solid points) and bovine (hollow points) (courtesy: Vashishth *et al.*[64]), (b) bovine bone (courtesy: Pezzotti and Sakakura[67]), (c) equine bone (courtesy: Malik *et al.*[66]), and (d) human bone tested in Hanks' Balanced Salt Solution (HBSS) (courtesy: Nalla *et al.*[49,70,71]). Note the initial rising R-curve behaviour in each case (supporting the existence of active extrinsic toughening mechanisms), although subsequent behaviour may differ.

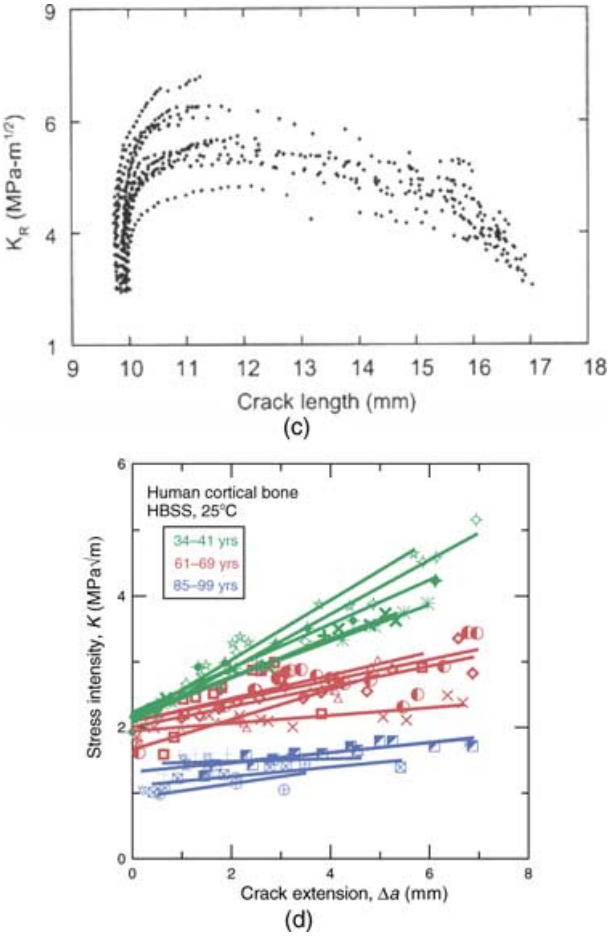

Fig. 7 Continued.

initiation toughness and the (initial) slope, respectively. Similarly, Malik *et al.*[66] observed rising R-curve behaviour for transverse crack growth in equine bone (Fig. 7c); here R-curves reached a steady-state plateau, and in some cases decreased, with mean K_o values of ~4.38–4.72 MPa$\sqrt{}$m, and mean slopes (calculated from Ref. [66]) of 1.06–2.57 MPa$\sqrt{}$m/mm. Additionally, linearly rising R-curve behaviour, with no apparent plateau, has been reported for cortical bone from red deer antler.[68]

Recent R-curve investigations using human cortical bone, by Nalla *et al.*[49,70,71] involved longitudinal (proximal-distal) crack growth, using the C-L orientation, in humeral bone grouped into three age groups (Fig. 7d). Average crack-initiation toughness, K_o, values of 2.07, 1.96 and 1.26 MPa$\sqrt{}$m, with mean slopes of 0.37, 0.16 and 0.06 MPa$\sqrt{}$m/mm, were observed with the R-curves monotonically rising over 5–7 mm (no plateau) for the *Young* (donor age: 34–41 years), *Middle-Aged* (donor age: 61–69 years) and *Aged* groups (donor age: 85–99 years), respectively. These data are plotted in Fig. 8, together with the results of Vashishth *et al.*[64] and Wu and Vashishth[72] on human tibial and femoral bone, and clearly indicate that the toughness of bone declines with age. (Although it is possible that anatomical location (tibia and femur *vs.* humerus) may affect the steepness of the decline.) Specifically, there is not only a decrease in the initiation toughness with age, but also a decrease in the crack-growth toughness.

While the initiation toughness does decrease, the effect of ageing is most apparent on the growth toughness, which declines to nearly zero in the case of the very elderly. These trends are clearly evident in Fig. 8 where the crack-initiation toughness decreases ~40% over six decades from 40 to 100 years, while the growth toughness

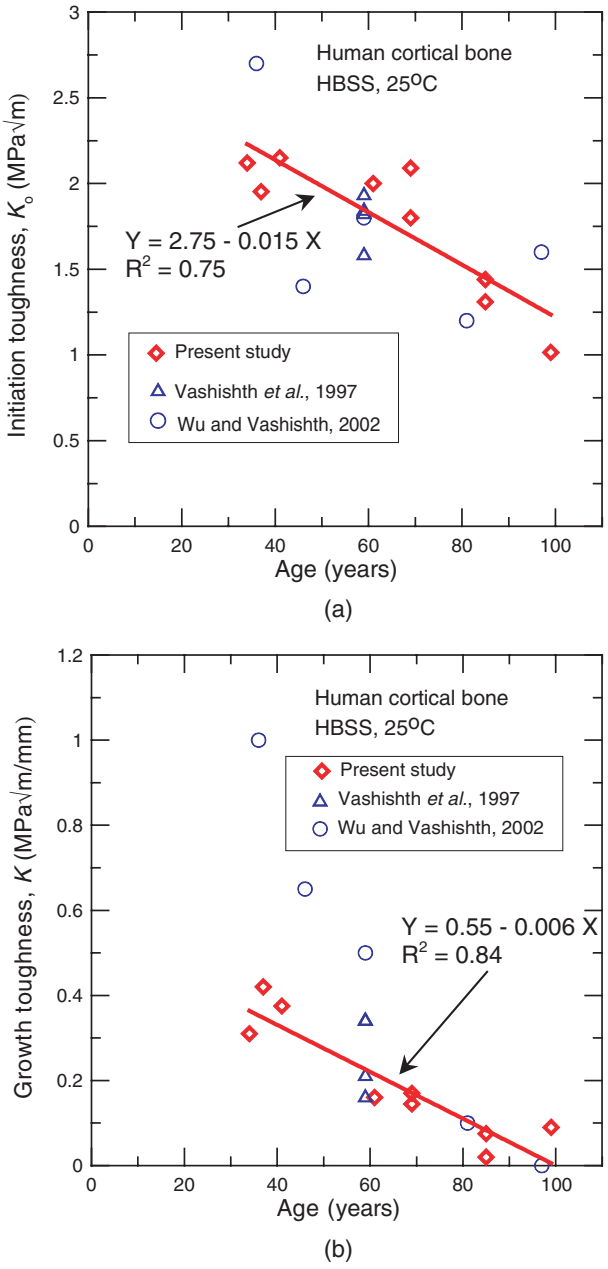

Fig. 8 Variation in the (a) crack-initiation toughness, K_o, and the (b) crack-growth toughness (slope of the R-curve) with age for human cortical bone. A linear regression of the data is shown in each case for the data of Nalla *et al.*[49,70,71]; fit equation and coefficient of determination, R^2, is also included. Data from Vashishth *et al.*[64] and Wu and Vashishth[72] are also plotted for comparison (not included in regression).

is essentially eliminated over the same age range. Such deterioration in the fracture resistance with age is consistent with the trend observed in studies that report single-value toughnesses.[19,22,24,27,28,36,38,52–56,73] Mechanistic reasons behind this age-related deterioration in the toughness of human cortical bone are described in the following section.

MECHANISTIC ASPECTS OF FRACTURE

Intrinsic mechanisms of fracture

In order to accurately model the fracture behaviour of bone, it is important to know whether the critical fracture event is stress- or strain-controlled, that is, whether fracture occurs when some critical strain or stress is locally achieved. While models for bone fracture have often assumed strain-controlled fracture,[74–76] recently, experiments were conducted by Nalla *et al.*[37] to verify this hypothesis using the double-notched four-point bend geometry (Fig. 9). With this geometry, since there is a constant bending moment between the inner two loading points, both notches experience the same stress and displacements; thus, when one notch breaks, the other is 'frozen' just at the point of unstable fracture.[1] Moreover, in the presence of some degree of inelasticity, the maximum stresses peak ahead of the notch near the elastic–plastic interface, whereas the maximum strains peak at the notch root; consequently, the location of the initial cracking events just prior to fracture are an indicator of whether fracture initiation is stress- or strain-controlled (see Ref. [37] for a details). These experimental studies showed that the onset of the *local* fracture events in cortical bone is consistent with strain-controlled fracture by noting that crack initiation occurred at points of maximum strain, that is, directly at the notch root, as opposed to points of maximum stress.

At present, further information on the intrinsic micromechanisms of fracture in bone is largely unavailable; however, as mentioned previously, the cement lines are thought to provide an intrinsically weaker path for fracture relative to the rest of the microstructure. This weak path most likely plays a strong role in the orientation effect seen in the fracture of bone (Fig. 4), where cortical bone demonstrates lower intrinsic toughness in orientations where the crack can run along the cement lines.

[1]There is a question in inhomogeneous materials such as bone whether the microstructure beneath the two notches is sufficiently similar for this test to work. This is a statistical sampling problem, and one solution is to perform many experiments. However, in actuality, ahead of a blunt notch, the volume of material 'sampled' (i.e. the active volume associated with the fracture process) is many orders of magnitude larger than ahead of a sharp (e.g. fatigue) crack. Indeed, in bone the maximum stresses ahead of a rounded notch peak hundreds of micrometres ahead of the notch tip, that is, over dimensions far larger than the characteristic structural dimensions, compared to an atomically sharp crack where the stresses peak at a location roughly two order of magnitude closer to the tip. Hence, notched tests are in many respects more 'reliable' than conventional sharp-crack tests for such inhomogeneous materials because they 'sample' far larger volumes of material, in the case of bone over dimensions larger than the microstructural inhomogeneities.

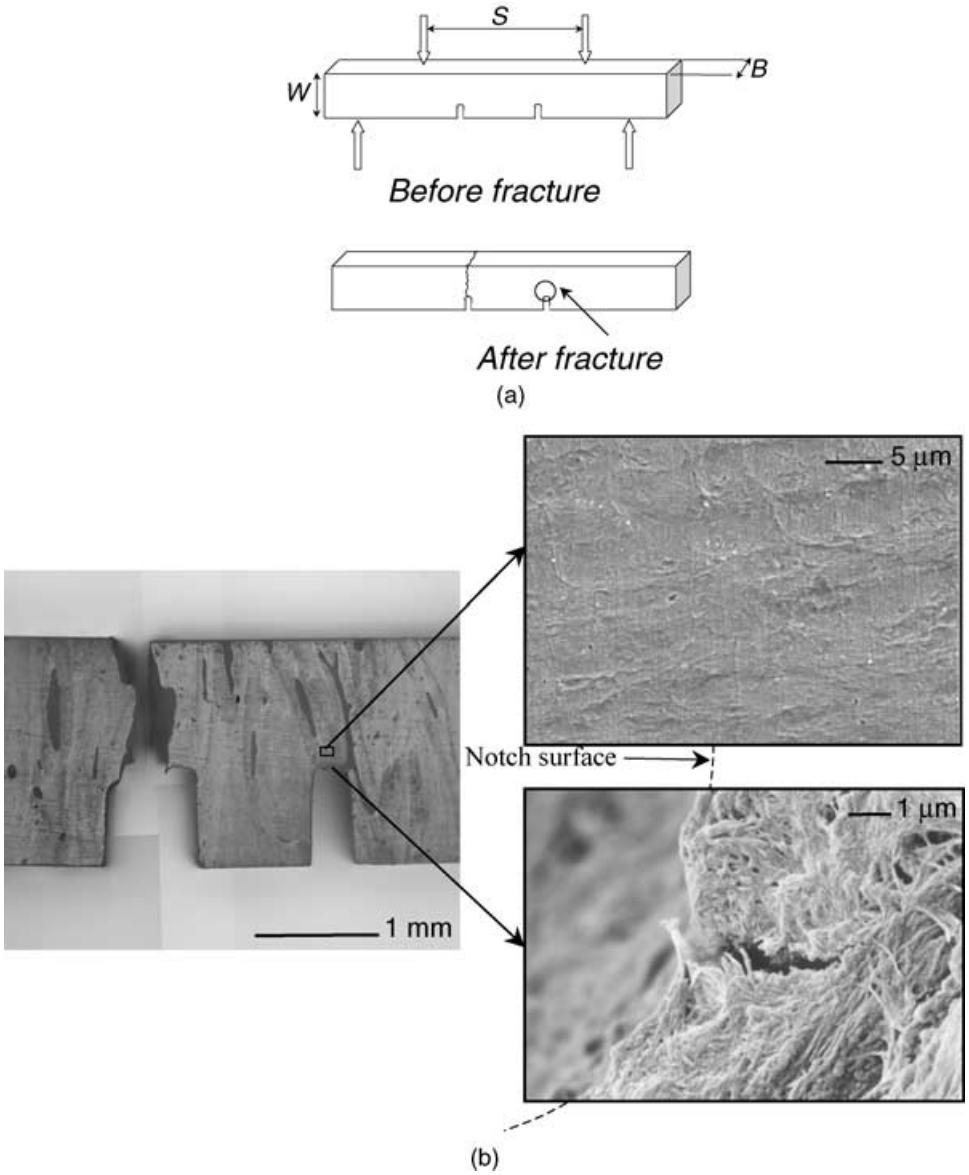

Fig. 9 (a) Schematic illustration of the double-notched four-point bend test used to discern whether fracture is stress- or strain-controlled. Between the inner two loading points, the bending moment is constant; thus, when one notch breaks, the other is "frozen" at a point just prior to fracture instability. The region beneath this unbroken notch (as indicated by the encircled area) is then carefully examined to determine the site of the precursor microscopic events involved in the fracture process. (b) Optical micrographs (left) of typical double-notch specimens after fracture, together with scanning electron micrographs (right) of the area of interest for the purpose of determining the failure criterion. Note the absence of crack initiation at the location of maximum stress as illustrated for the C-L (proximal-distal) orientation (top, right), supporting a strain-controlled local fracture criterion.[84]

Thus, one key to further understanding the intrinsic failure micromechanisms of cortical bone may lie in understanding the specific structural differences between the cement lines and the other parts of the bone tissue.

Extrinsic toughening mechanisms

Significant progress has been made in understanding the extrinsic toughening mechanisms in bone, which are responsible for the rising R-curve behaviour. Extrinsic toughening mechanisms (Fig. 6) act primarily behind the crack tip, in the surrounding material and/or in the crack wake, and cause a local reduction in the stresses to be felt at the crack tip, as compared to cases where such mechanisms are absent. Early studies attributed the rising toughness with crack extension observed in bone to the mechanism of constrained microcracking;[64,65,68] however, more recently it has been argued that crack bridging

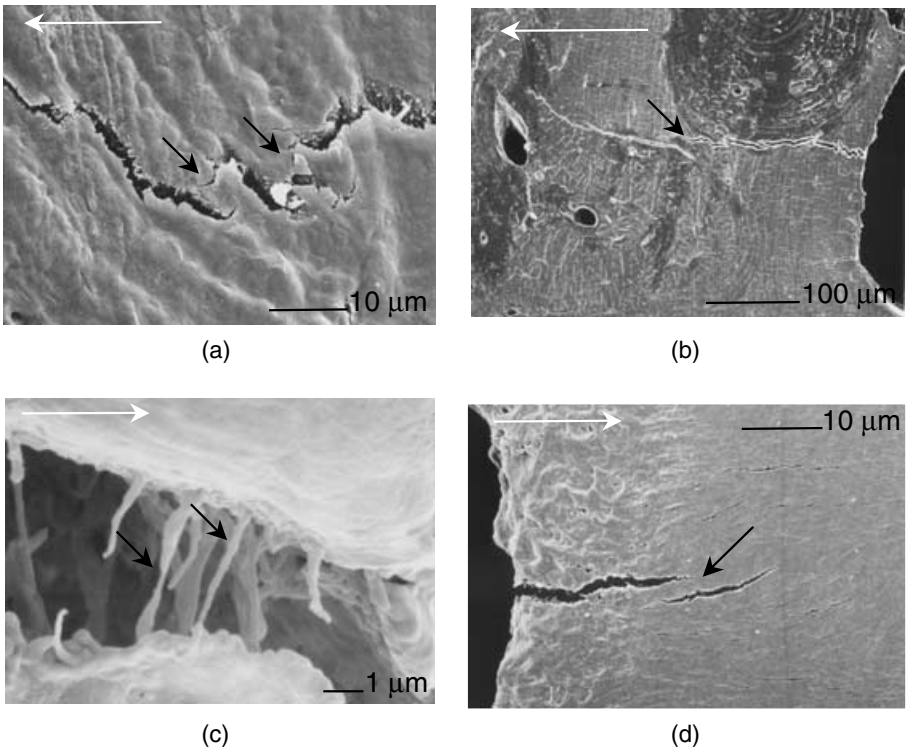

Fig. 10 Scanning electron micrographs illustrating crack bridging. For the transverse (radial) orientation, (a, b) evidence of uncracked-ligament bridging (indicated by black arrows), and (c) possible collagen fibril-based bridging (indicated by black arrows). For the longitudinal orientation, (d) evidence of uncracked-ligament bridging (indicated by black arrow). The white arrows in (a)–(d) indicate the direction of nominal crack growth (courtesy: Nalla *et al.*[84]).

is in fact the primary mechanism responsible for such behaviour,[37,49,67] where intact bridges of material across the crack sustain part of the applied load (Fig. 10). Because individual microcracks (cracks of the order of the microstructural features in size) may lead to the creation of bridges, primarily by forming ahead of the crack tip and imperfectly linking with the tip, it is important to understand the differences in the mechanics involved with each mechanism. With constrained microcracking, the formation of a diffuse microcracked damage zone ahead of the crack tip, which remains in the wake of the crack as it extends, is reasoned to increase the (extrinsic) toughness due to (1) the volume expansion within the damage zone from the formation of microcracks, which if constrained by surrounding rigid material exerts a compressive stress at the crack tip, and (2) the reduction in modulus that occurs within this zone.[77,78] Counteracting these extrinsic toughening benefits, at least in part, is the fact that a microcracked region ahead of the crack that can act to lower the intrinsic toughness, as has been observed in highly microcracked bone.[79] Thus, the extrinsic toughening benefits need to be high for this mechanism to be effective, and in general, the toughening effects of constrained microcracking are small, causing it to be largely discounted as a significant source of toughening in all but a few multiphase ceramic materials with high internal residual stresses.[60,80]

In contrast, crack bridging involves regions of uncracked material spanning the crack wake and sustaining part of the applied load that would otherwise contribute to crack growth. In bone, this bridging occurs in the form of so called 'uncracked ligaments', often hundreds of micrometers in size, or by individual collagen fibrils over much smaller dimensions.[49,67,70,81] Such uncracked regions are left in the crack wake as a result of either non-uniform advance of the crack front and/or by the imperfect linking of microcracks, which initiated ahead of the crack tip, with the main crack. Although individual microcracks may lead to bridge formation, the mechanics of the two mechanisms are quite distinct. Crack bridging acts to reduce the stress intensity experienced at the crack tip, K_{tip}, relative to the applied stress intensity, K_{app}, by an amount typically referred to as the bridging stress intensity, K_{br}, viz:[61–63]

$$K_{\text{tip}} = K_{\text{app}} - K_{\text{br}}. \tag{5}$$

The reduction in stress intensity is due to the fact that bridges in the crack wake sustain a portion of the applied load. Because bridges develop with crack extension, K_{br} increases with crack extension as well, resulting in rising

R-curve behaviour. A steady-state 'plateau' toughness may be reached under conditions where bridges are created and destroyed at the same rate, at which point K_{br} essentially becomes constant.

Uncracked-ligament bridges appear to provide the majority of extrinsic toughening which contributes to R-curve behaviour in cortical bone,[49,70] while collagen fibre bridging is hypothesized to play a role in resisting the propagation of microcracks.[81] Because crack bridging should decrease the measured compliance of a fracture mechanics specimen (i.e., increase stiffness), whereas a diffuse microcrack zone should marginally increase the compliance (decrease stiffness) (Fig. 11a), Nalla *et al.*[70] demonstrated that since experimental data showed a reduction in the measured compliance (Fig. 11b), crack bridging is thought to be the dominant extrinsic toughening mechanism in human cortical bone. Indeed, based on theoretical calculations, unrealistically high microcrack volume fractions (~60 to 90%) would be needed to account for the levels of extrinsic toughening seen;[70] such microcrack densities are far in excess of those experimentally measured in bone, for example, by Vashishth *et al.*[64] which were on the order of ~3%.

For human and bovine bone, both collagen fibre bridges near the crack tip, and uncracked-ligament bridges far into the crack wake have been readily observed using microscopy (Fig. 9) and X-ray tomographic techniques (Fig. 12).[37,49,67,70] Characterization of the uncracked-ligament bridging, which is of much larger size scale, has revealed that in human humeri, such bridging zones can extend some 5–6 mm behind the crack tip and sustain substantial stresses.[49] Quantitative estimates of the contribution of bridging to the toughness was made using experimental compliance data.[49,70] Furthermore, average (through-thickness) peak bridging stresses have been calculated to be in the range from 7 to 17 MPa near the crack tip, and to decay over distances of 5–6 mm within the bridging zones in the crack wake.[49] Pezzotti and Sakakura[67] used Raman microprobe spectroscopy to measure bridging stresses over a distance of 100 μm behind a crack tip in bovine femur and reported stresses as high at 200–300 MPa within the first 10 μm of the crack tip, but falling off to ~10–50 MPa at a distance of 100 μm behind the tip. Such results gave highly localized measurements, with a 1 μm probe diameter, measuring to a depth of 20 μm. The higher bridging stresses deduced in the latter study may in part be due to species variation; however, by considering only highly localized measurements, they probably result from the fact that bridges are discrete entities, and while the stresses may be very high locally, this is offset by surrounding unbridged regions unable to support any load.

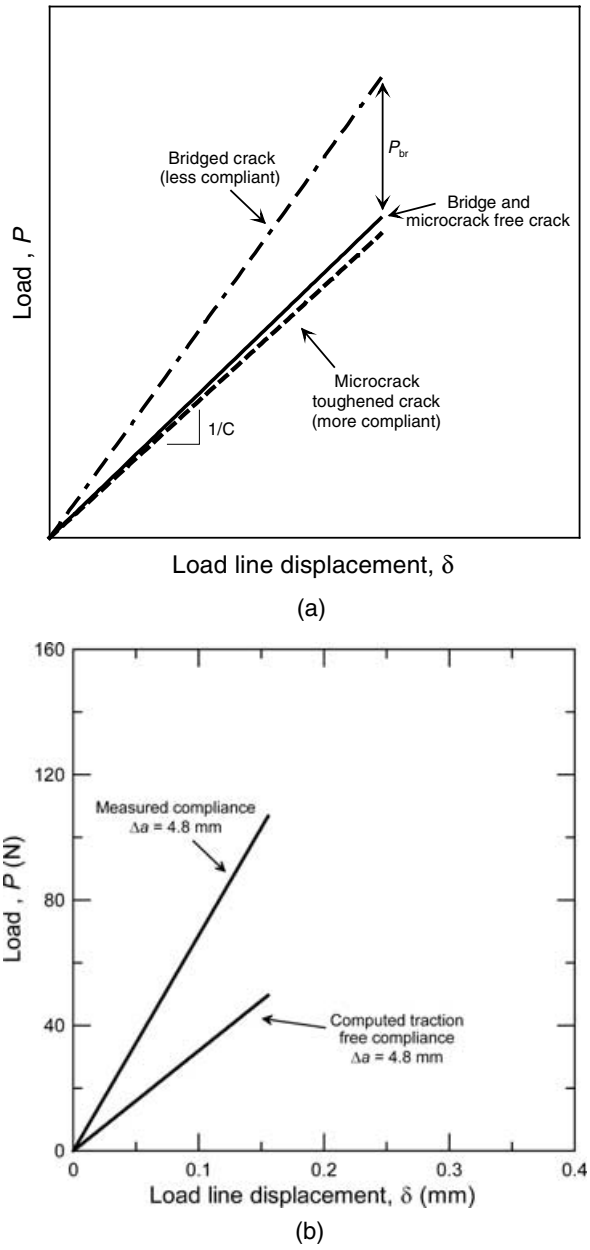

Fig. 11 (a) Schematic illustration of the variation in compliance, C, of a sample containing a crack of given size with the mechanism of toughening. Compared to the theoretical compliance of a linear-elastic traction-free crack, the role of crack bridging is to lower the compliance (i.e., to increase the stiffness), whereas microcracking will tend to slightly elevate the compliance (i.e., to lower stiffness). (b) Comparison of the *experimental* (measured) and *theoretical* (bridge- and microcrack-free) compliance curves. Note that the measured compliance is distinctly lower than the bridge- and microcrack-free compliance, which provides strong evidence of the role of crack bridging, as opposed to microcracking, in the toughening of human cortical bone.[49,70]

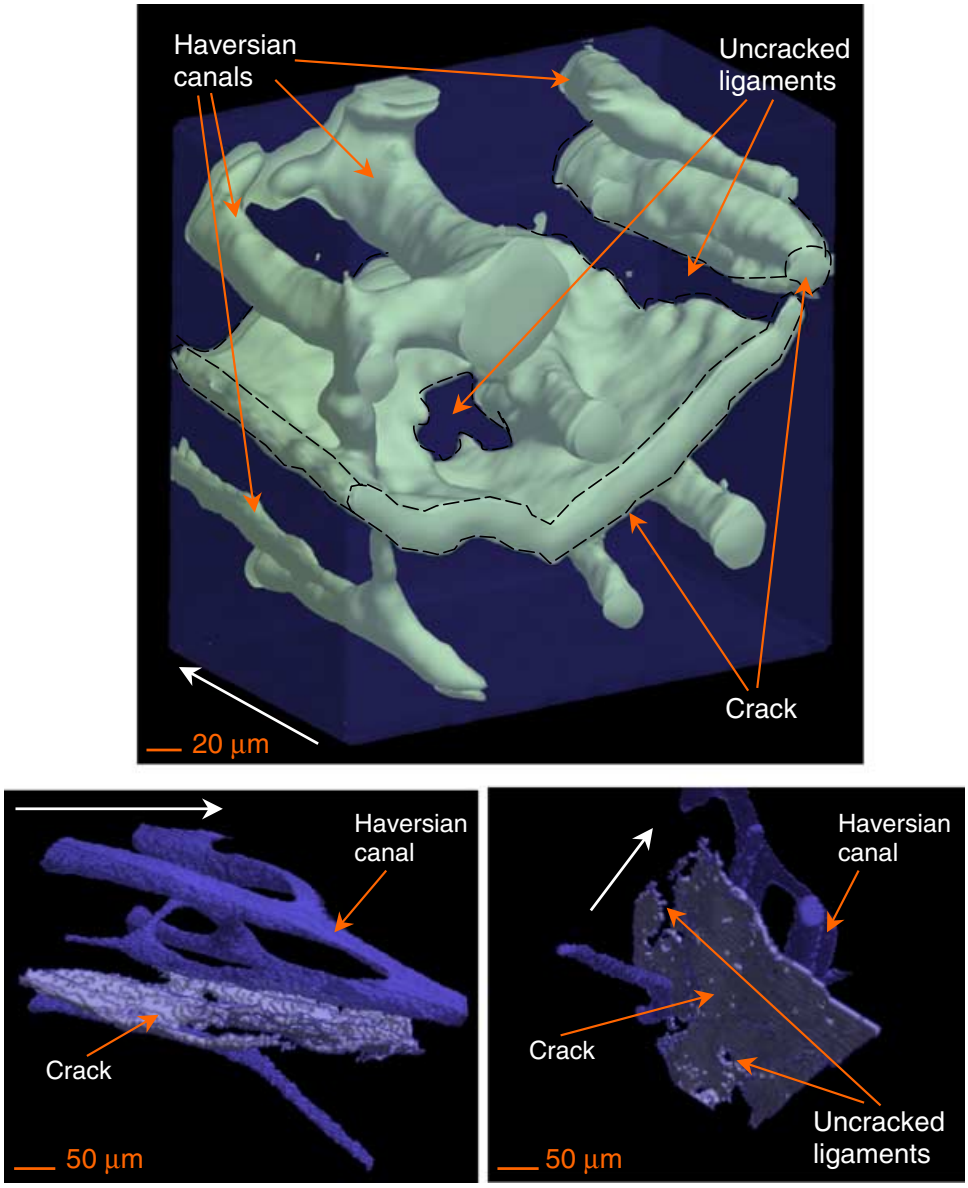

Fig. 12 Three-dimensional tomographic reconstructions (5 μm voxel size/resolution) of sections of a crack grown in the longitudinal orientation are shown. Note that the crack appears to follow the cement lines bordering the osteons. Uncracked ligaments are indicated by the orange arrows. The white arrow in each case is the direction of nominal crack growth (courtesy: Nalla *et al.*[49]).

Estimates based on theoretical models have also been made for the contributions from various toughening mechanisms. The highest toughness was observed in the L-C (transverse) orientation; here the crack path deflects at $\sim 90^{\circ}$ to the plane of maximum tensile stress (Fig. 4c). The effect of this deflection is to substantially increase the fracture resistance, as shown by the following analysis. Assuming, for the sake of simplicity, that these deflections/kinks represent in-plane tilts through an angle, α, to the crack plane, then the local mode-I and mode-II stress intensities, k_1 and k_2, at the deflected crack tip are given by:[82,83]

$$k_1(\alpha) = c_{11}(\alpha)K_{\mathrm{I}} + c_{12}(\alpha)K_{\mathrm{II}},$$
$$k_2(\alpha) = c_{21}(\alpha)K_{\mathrm{I}} + c_{22}(\alpha)K_{\mathrm{II}}, \qquad (6)$$

where K_{I} and K_{II} are, respectively, the mode-I and mode-II far-field stress intensities for a main crack, and the coefficients, $c_{ij}(\alpha)$, are mathematical functions of the deflection angle, ($\alpha \sim 90^{\circ}$).[82–84] The effective stress intensity at the tip of the deflected crack tip, K_{d}, can then be calculated by summing the mode-I and mode-II contributions in terms

of the strain-energy release rate, viz:

$$K_d = \left(k_1^2 + k_2^2\right)^{1/2}. \quad (7)$$

For the example given in Fig. 4 for a nominally tensile loaded crack, where $K_I = 5.33$ MPa$\sqrt{}$m and $K_{II} = 0$, the value of the stress intensity at the crack tip is reduced locally by ~50% due to such deflection to ~2.7 MPa$\sqrt{}$m, compared to that for an undeflected crack.[84] This calculation is consistent with the effective toughness being approximately twice as high in this orientation as compared to the C-R and C-L (longitudinal) orientations (Fig. 4a).

In the C-L (proximal-distal) and C-R (medial-lateral) orientations, crack bridging appears to be the prominent source of toughening, as was discussed previously in this section. Theoretical estimates of bridging due to uncracked ligaments in the latter (C-R) orientation can be made based on a limiting crack-opening approach:[85]

$$K_{br} = -f_{ul}K_I[(1 + l_{ul}/rb)^{1/2} - 1]/ \\ [1 - f_{ul} + f_{ul}(1 + l_{ul}/rb)^{1/2}], \quad (8)$$

where f_{ul} is the area-fraction of bridging ligaments on the crack plane (~0.2–0.4, from crack-path observations), K_I is the applied stress intensity (~2.4 MPa$\sqrt{}$m), l_{ul} is the bridging-zone size (~50–300 μm, from crack-path observations), r is a rotational factor (0.20–0.47) and b is the remaining (unbroken) ligament. Again, substituting typical values for these parameters for human humeri,[84] a contribution to the toughness on the order of K_{br} ~0.3 MPa$\sqrt{}$m was obtained for the C-R orientation. Similar analyses for the C-L orientation yielded even higher values of ~1–1.6 MPa$\sqrt{}$m due to the larger (~5 mm) bridging zones in this orientation.

For toughening associated with bridging by collagen fibrils, the uniform-traction Dugdale-zone model[86] can be employed to estimate the resulting decrease in the stress intensity, K_b^f, due to 'fibre-bridging', viz:

$$K_b^f = 2\sigma_b f_f(2l_f/\pi)^{1/2}, \quad (9)$$

where σ_b is the normal bridging stress on the fibres (~100 MPa), f_f is the effective area-fraction of the collagen fibres on the crack plane (~0.15, from crack-path observations) and l_f is the bridging-zone length (~10 μm, from crack-path observations). Using these parameters estimated for human humeri, a value of $K_b^f \sim 0.08$ MPa$\sqrt{}$m can be obtained for both longitudinal (C-R and C-L) orientations where such bridging was observed, suggesting that bridging by individual collagen fibres contributes little to the toughness of bone.[84] However, this mechanism might be expected to be significant for individual microcracks, where due to the substantially smaller size scales collagen fibre bridges would be able to span a larger percentage of the crack length.

Finally, based on accepted models for microcrack toughening due to dilation and modulus reduction,[78,87,88] the increase in toughness due to microcracks can be expressed as:

$$K_m = 0.22\varepsilon_m E' f_m\sqrt{l_m} + \beta f_m K_c, \quad (10)$$

where ϵ_m is the residual volumetric strain (= 0.002, as calculated from data in Ref. [88]), E' is the plane-strain elastic modulus, f_m is the volume-fraction of microcracks, l_m is the height of the microcrack zone, β is a factor dependent on Poisson's ratio (~1.2).[88] Using a volume fraction, $f_m \sim 3\%$ from the observations of Vashishth *et al.*[64] for the C-L orientation in human tibia, the contribution to the toughness from microcracking would be ~0.1 MPa$\sqrt{}$m; similar values are obtained for the other orientations. Based on such simple theoretical modelling for quantification, the dominant toughening mechanisms in bone appear to be (1) crack deflection along the cement lines in the L-C (transverse) orientation, and (2) crack bridging by uncracked ligaments in the C-R and C-L (longitudinal) orientations. The roles of collagen fibril bridging and microcracking appear to be relatively insignificant. Based on this appreciation of the toughening mechanisms in bone, the anisotropy in the fracture toughness of bone with orientation can be understood in terms of a large contribution from crack deflection in the transverse orientation as compared to a smaller contribution from crack bridging in the longitudinal orientations.

With regard to ageing effects on crack bridging, R-curve results show a clear decrease in the extrinsic toughening contribution (i.e. K_{br}) for older bone, as shown in Figs 7 and 8. Mechanistically, given that there are increased levels of remodelling of bone with age, one may reason that the higher density of secondary osteons (and hence, weak cement lines that may fail prematurely ahead of a growing crack) could lead to a more extensive ligament bridging zone. Alternatively, bridge formation may be easier due to increased crack branching along the greater number of cement lines, where bridges are left in the crack wake due to the imperfect linking of the branches. In both cases, although bridge formation may be easier, the bridging zones likely would comprise smaller bridges. Whether a larger amount of smaller bridging elements might lead to increased toughening is unclear; however, experimental observations demonstrate smaller bridges (Fig. 13), and less extrinsic toughening (Figs 7d and 8b). Furthermore, the quality of the collagen forming such bridges may play an important role as well. Poorer collagen quality might lead to weaker bridges and could well be expected to offset any increased propensity for bridge formation in older bone, leading to fewer and smaller bridges as is suggested by typical two-dimensional through-thickness tomographic 'slices' of cracks in bone of two different ages (Fig. 13). Indeed, collagen molecule

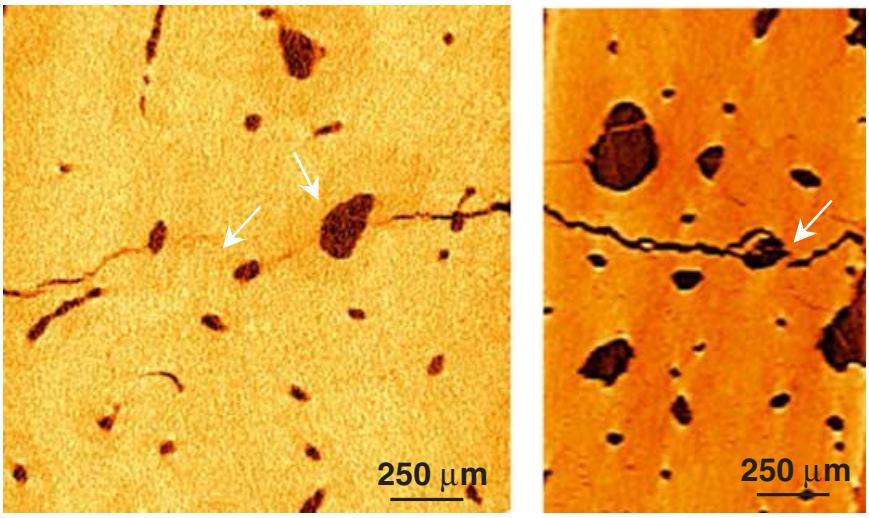

Fig. 13 Two-dimensional reconstruction slices showing typical cracks in specimens taken from the (a) *Young* and (b) *Aged* groups (see Fig. 7d). Note the much smaller uncracked-ligament crack bridges (indicated by white arrows) in the older bone as discussed in detail elsewhere.[71] The direction of crack propagation is into the page.

integrity has been previously implicated in the deterioration of mechanical properties of demineralized bone,[89] which is presumed to be indicative of behaviour in mineralized bone. As the microstructural factors affecting crack initiation and growth in most materials are invariably quite distinct,[61–63] the challenge is to identify *and quantify* the specific mechanisms affecting each process in terms of the changes that occur in the micro/nano-structure of bone with age. It is apparent that there is still much to be determined, and both quantitative and qualitative assessments of bridging are currently being undertaken in order to achieve an improved mechanistic understanding of the role of ageing on bone fracture.

TIME-DEPENDENT FRACTURE

Sustained-load cracking

Similar to many structural materials, human bone can fail subcritically, that is, by slow crack growth at stress intensities less than the fracture toughness, under both sustained and cyclically varying loads. Subcritical cracking is considered to be of key importance in understanding so-called 'stress fractures',[2,5,31,79,90–113] where a fracture occurs (presumably by sustained-load cracking or more likely cyclic fatigue) due to an increased period of loading, instead of by a critical fracture event. Sustained-load cracking, that is, subcritical cracking under sustained quasi-static loading, is probably of less clinical significance than true fatigue loading since elevated loading patterns that lead to stress fractures are often cyclic in nature. Such behaviour is of importance, however, when considering the mechanisms of subcritical crack growth. Indeed, many engineering materials, such as glasses and brittle ceramics, exhibit subcritical crack growth under cyclic loading as the result of discrete (static) cracking events, where unloading essentially plays no role.[114]

Bone does show subcritical cracking under sustained (non-cyclic) loads. Early results on bovine tibia demonstrated that cracks grew in the longitudinal direction at higher velocities ($\sim 10^{-5}$–10^{-3} ms^{-1})[33,115,116] as the driving force (K or G) was increased. Attempts to grow cracks at faster rates resulted in catastrophic failure, along with a change in fracture morphology and a lower toughness. More recent studies[49] on human humeri, also in the longitudinal (C-L) direction, report similar results but over a much wider range of growth rates from $\sim 10^{-9}$ to 10^{-4} ms^{-1}; again higher stress intensities were needed to grow cracks at higher growth rates (Fig. 14). Although in engineering materials such behaviour is typically associated with environmental effects, it is unclear what role, if any, the physiological environment plays in subcritical cracking behaviour of cortical bone. A striking feature observed in cortical bone, however, is that at growth rates below $\sim 10^{-9}$ m/s, significant crack blunting occurs which eventually leads to crack arrest (Fig. 15).[49] Thus, even without remodelling, bone has a mechanism to arrest the growth of subcritical cracks driven by static (non-cyclic) loads.

Fatigue behaviour

Cyclic loading can also lead to subcritical crack growth; indeed, fatigue failures have been studied quite extensively in

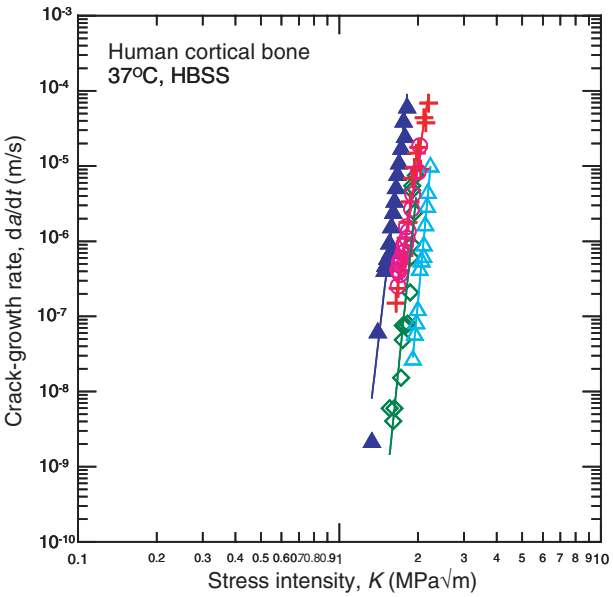

Fig. 14 Results showing the time-dependent subcritical crack-growth behaviour of human cortical bone, in terms of the growth rates, d*a*/d*t*, as a function of the stress intensity, *K*, for growth rates $>10^{-9}$ ms^{-1}. Different data sets refer to the results from five separate test samples. Testing was performed in 37 °C Hanks' Balanced Salt Solution (HBSS). Attempts at acquiring data for growth rates less than 10^{-9} m^{-1} were unsuccessful owing to substantial crack blunting over the time scales involved (courtesy: Nalla *et al.*[49]).

cortical bone.[2,5,31,79,90–113] Fatigue behaviour can be characterized either in terms of total life, as measured using stress or strain versus life (*S/N*) curves, or solely in terms of the crack propagation life, where fracture mechanics is used to provide a basis for the so-called damage-tolerant analysis. Both approaches are described below.

Stress-life approach

One traditional approach to fatigue failure is to characterize the total life to failure of nominally flaw-free, 'smooth-bar' specimens, as a function of the alternating stress; this is termed the *stress-life* or '*S/N*' approach. With this method, the measured fatigue lifetime represents the number of the cycles both to initiate and to propagate a (dominant) crack to failure. Such an approach has been widely used for fatigue studies on cortical bone to investigate a wide variety of issues, including age,[99] donor species,[100] cyclic frequency,[31,93,107,117] testing geometry,[31,99,103] loading mode,[98,106,112] fatigue-induced damage accumulation[79,98–100,108] and its role in inducing *in vivo* repair (remodelling) and adaptation.[4]

Fatigue lifetimes show a reduction with increasing age, as suggested by the data of Zioupos *et al.*[99] who reported higher fatigue lifetimes for human femoral bone taken from a 27-year old as compared to a 56-year old donor (Fig. 16a). The same authors also showed that bovine femoral bone is stronger in tensile fatigue than red deer antler (Fig. 16b).[100] Additionally, data for bovine and human bone from other studies are shown in Fig. 16. Frequency affects *S/N* behaviour such that higher fatigue-cycle lifetimes are associated with higher frequencies.[93,107,117] Loading mode and test geometry have also been reported to have an effect on fatigue lifetimes. Zero-compression loading generally gives only slightly higher lifetimes (10–15%) than zero-tension loading,[117] although data from Pattin *et al.*[98] suggest there is a higher critical threshold for damage accumulation during fatigue under compressive loading (4000 $\mu\varepsilon$ vs. 2500 $\mu\varepsilon$). Vashishth *et al.*[106] reported a reduction in fatigue lifetimes when torsional loading was superimposed on tension–compression axial loading; similar results were seen for torsion as compared to compressive axial loading.[112] These differing variables often make direct comparisons of results from different species difficult; however, data from Swanson *et al.*[91] for human bone and from Carter and Caler[94] for bovine bone suggest that human bone is weaker than bovine bone in fatigue. Because most data for human bone are from aged donors, however, the effects of age may play a stronger role than species variation.[5]

Test geometry also has an effect on fatigue life, which is a disadvantage of the *S/N* approach to fatigue. For example, three-point bending has been claimed to induce less stiffness loss (reflective of fatigue damage) as compared to four-point bending;[103] data in Ref. [99] further suggest that fatigue lifetimes in human bone are progressively decreased by testing in (four-point) bending, rotating cantilever, and zero-tension loading. Both these latter studies presumably reflect that fatigue damage will accumulate more readily in test geometries with larger statistical 'sampling' volumes (the reader is referred to Ref. [5] for further details on statistical sampling in fatigue). These reported results of the fatigue of bone are, on the whole, in line with the typical fatigue behaviour displayed by most common engineering materials,[118] although variations in parameters, such as temperature, donor age, etc., can complicate comparisons between different studies.

Despite the fact that there is an extensive body of literature reporting *S/N* fatigue data, it is difficult to ascertain information about the mechanisms of fatigue failure from such data. Accordingly, a number of studies have looked at the accumulation of microdamage in bone. Microdamage accumulation in bone by fatigue has been acknowledged for more than 40 years,[45,119] and a number of recent studies have looked at methods of imaging such damage,[120–122] how fatigue cycling can induce it,[79,98–100,108] the loss in mechanical properties due to such damage[79,98] and the role of damage in triggering remodelling *in vivo*.[4] An excellent review on this topic may be found elsewhere.[5]

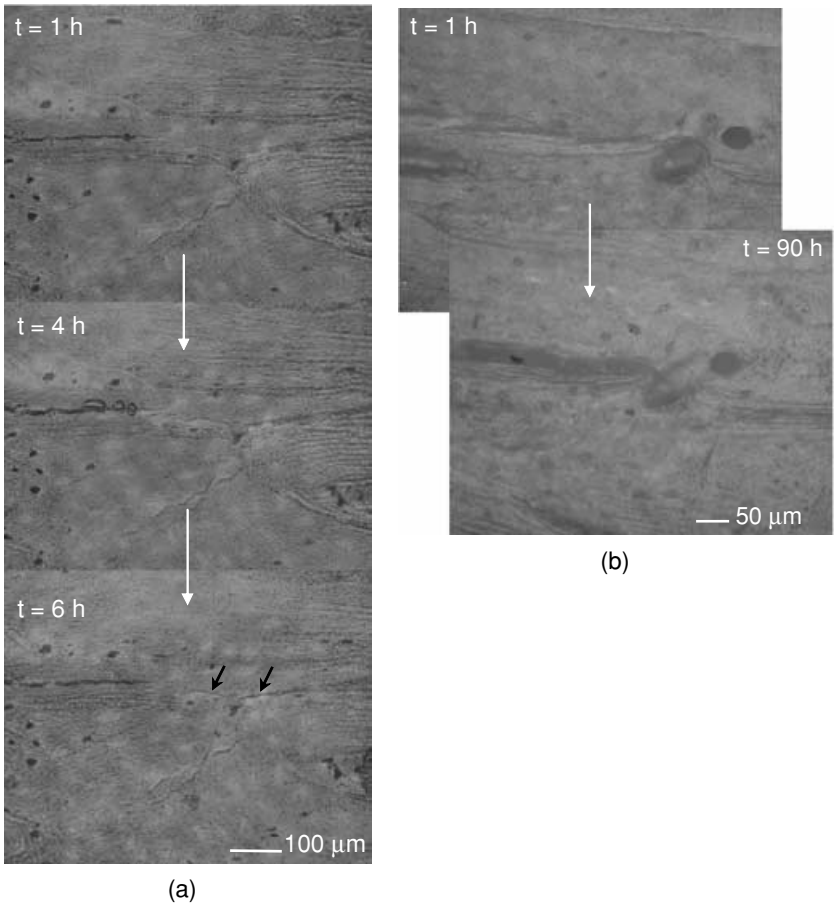

Fig. 15 Time-elapsed optical micrographs showing the (a) time-dependent crack extension (clearly seen in bottom micrograph, as indicated by black arrows) that occurs over a time scale of several hours, and (b) time-dependent crack blunting behaviour in human cortical bone as evidenced by the larger crack opening in the lower panel. Note also the evidence of uncracked-ligament bridging and the lack of crack blunting on the shorter time scale in (a). The direction of nominal crack growth is from left to right (courtesy: Nalla *et al.*[49]).

One critical mechanistic issue is whether fatigue damage is time- or cycle-dependent (or indeed both). One approach to address this issue has been to examine the role of test frequency on *S/N* behaviour—a time-dependent mechanism is implied if the times-to-failure for different test frequencies are identical. Such studies, from Caler and Carter,[117] Lafferty and Raju,[93] and Zioupos *et al.*[107], suggest that tensile fatigue in bone can be time-dependent, since when plotted with respect to time, the effect of test frequency (0.002–2 Hz,[117] 30–125 Hz,[93] and 0.5–5 Hz[107]) on the fatigue lifetimes is essentially eliminated.[5,107] To explain these observations, Carter and Caler,[123] and subsequently Taylor,[5] have suggested that the fatigue process in bone may involve contributions from both static and cyclic loading induced fracture, and that there is a transition from a "creep"-dominated to a fatigue-dominated regime with decreasing stress levels; however, it is currently unclear whether true creep deformation, which does occur in bone at ambient temperatures,[124] contributes to this transition.

S/N results are not easy to interpret in terms of fatigue mechanisms, however, because failure times in fatigue include both the crack initiation and the propagation stages, which certainly involve separate mechanisms that may be affected by external variables in different ways. Furthermore, in bone, where there is typically an inherent population of flaws/cracks, the crack initiation life may be less important. For this reason, many recent studies on the fatigue of bone have concentrated instead on the crack propagation life.

Damage-tolerant approach

Crack propagation lives may be assessed using the *damage-tolerant* approach, a fracture mechanics methodology where the crack-propagation rate, da/dN, is assessed in terms of the range in stress-intensity factor, ΔK, defined as the difference between the stress intensity at the maximum and minimum of the loading cycle. Fatigue lives may then be determined from the number of cycles required

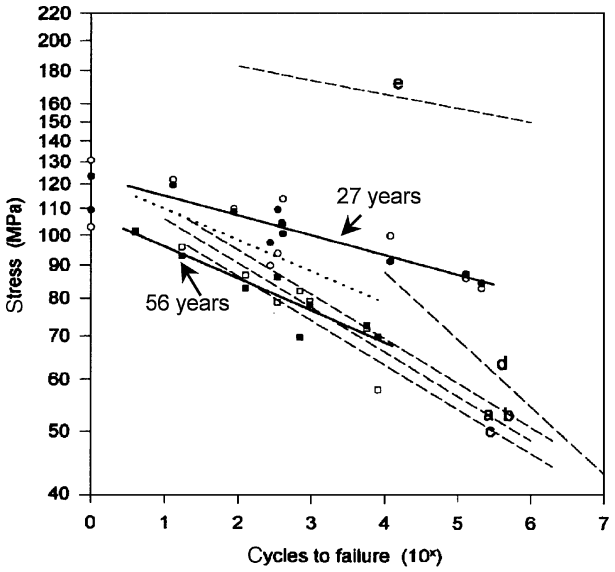

(a)

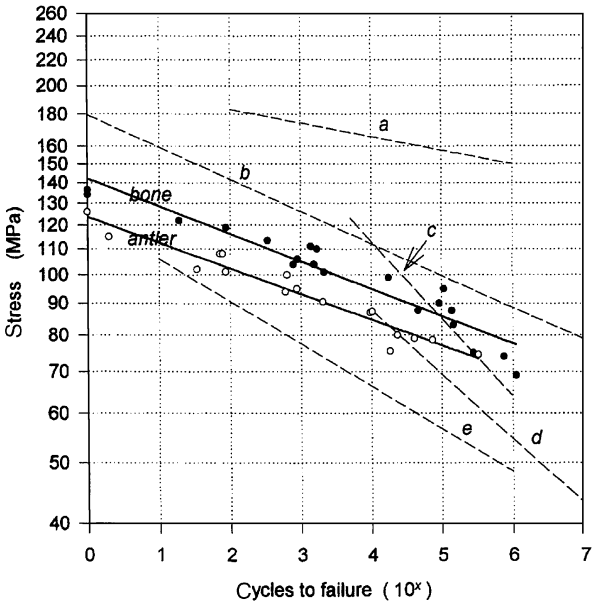

(b)

Fig. 16 Fatigue stress-life *S/N* data for bone. (a) The effect of age in reducing the fatigue lifetimes is evident (open symbols—raw data, closed symbols—modulus-corrected data). Dotted lines (marked a–e) show data from other studies (see ref. [100] for details). (b) The effect of species on fatigue lifetimes is shown. In addition to data for bovine femoral bone and red deer antler, dotted lines (marked a–e) show data from other studies: a,d,e—human, b,c—bovine (see Ref. [99] for details). (Courtesy: Zioupos *et al.*[99,100]).

for an incipient crack to grow subcritically to a critical size, as defined by the fracture toughness, using information relating da/dN to ΔK.[118] Wright and Hayes[125] first used this approach to characterize fatigue-crack growth in bovine bone using longitudinally oriented specimens to measure crack-growth rates for long cracks (i.e., cracks that are large as compared to the microstructural features of the underlying material) over growth rates of da/dN $\sim 7 \times 10^{-7}$ to $\sim 3 \times 10^{-4}$ m/cycle. These results were fitted to a simple Paris power-law formulation:[126]

$$da/dN = C'(\Delta K)^m, \tag{11}$$

where C' and m (Paris exponent) are scaling constants; values of m were found to be between 2.8 to 5.1. Although Wright and Hayes' data did suggest some effect of cyclic frequency on crack-growth rates, their results were not conclusive. Gibeling *et al.*[105] measured transverse crack-growth rates in osteonal equine bone of $\sim 6 \times 10^{-10}$ to $\sim 1 \times 10^{-5}$ m/cycle with a Paris exponent of $m \sim 10$.

For human bone, only one study has been reported to date; here Nalla *et al.*[113] measured exponent m values of ~4.4–9.5 for longitudinal fatigue-crack growth rates in Hanks' Balanced Salt Solution (HBSS) over a wide range from $\sim 2 \times 10^{-10}$ to $\sim 3 \times 10^{-5}$ m/cycle in human cortical bone taken from the humerus (Fig. 17). In agreement with *S/N* results, a transition from predominantly time-dependent cracking at higher ΔK values to a true fatigue (cycle-dependent) mechanism at lower ΔK values was reported, which can now be conclusively linked to the crack

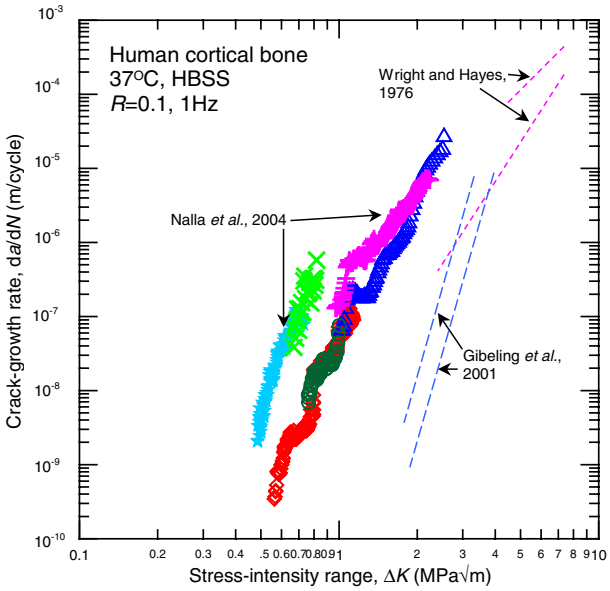

Fig. 17 Variation in *in vitro* fatigue-crack growth rates, da/dN as a function of the stress-intensity range, ΔK in 37 °C HBSS. Data shown as individual points are for crack growth in the longitudinal (proximal-distal) orientation in human humeral cortical bone (Nalla *et al.*[113]). Also included (as dotted lines) are data from Wright and Hayes[125] for longitudinal crack growth in bovine bone and from Gibeling *et al.*[105] for transverse crack growth in equine bone.

propagation stage of the fatigue life. Evidence of such a transition was provided through a series of novel three-step 'fatigue-sustained load-fatigue' experiments, with all three loading blocks performed at a fixed K_{max} value.[113] At higher growth rates ($K_{max} = 1.65$ MPa$\sqrt{m}$), the magnitude of the maximum stress was observed to be high enough to drive crack growth in the absence of fatigue cycling (Fig. 18a), while at lower growth rates ($K_{max} = 1$ MPa$\sqrt{m}$), crack growth was undetectable during the sustained-load portion, but restarted once the fatigue cycling was resumed (Fig. 18b). Such results strongly support the notion of a transition in the salient mechanisms responsible for subcritical crack growth in bone, from static-load (or 'creep') dominated to cyclic-load (fatigue) dominated mechanism(s), with decreasing growth rates and stress-intensity level.

Such a distinction can also be achieved based on the methodology devised by Evans and Fuller,[114] where the cyclic fatigue-crack growth rates are 'predicted' solely from sustained-load cracking data over the full range of K_{max} values (Fig. 14).[49] The predictions are for materials that show *no true cyclic fatigue effects*, that is, on the premise that there is no effect on crack extension specific to cyclic loading and that fatigue-crack growth is merely the sum of the increments of static-load cracking associated with the sustained loads in each loading cycle. Using the Evans and Fuller approach,[114] these sustained loads are determined by integrating (with respect to time) over the fatigue loading cycle in order to 'predict' crack-growth rates from static-crack growth data, viz:

$$\frac{da}{dN} = A\int_0^{1/f}\left[\frac{1}{2}(K_{max} + K_{min}) + \frac{\Delta K}{2}(\sin(2\pi f t))\right]^n dt, \tag{12}$$

where f is the cyclic test frequency, K_{max} and K_{min} are as previously defined, and A and n are the scaling constants as defined according by the power–law relation used to fit the static-crack growth data shown in Fig. 14:

$$da/dt = AK^n. \tag{13}$$

Thus, the 'predicted' cyclic fatigue-crack growth rate behaviour can be compared with that measured experimentally. If the 'predicted' and experimental growth rates correspond well, the inference is that no true cyclic fatigue effect exists (e.g., as seen in sapphire[127]); however, if at a fixed stress-intensity range the experimentally measured rates exceed the 'predicted' rates, then this implies that cycle-dependent fatigue mechanisms are active.

Such a comparison between experimentally measured fatigue-crack growth rates in human cortical bone with the Evans–Fuller 'predictions' made solely from sustained-load cracking data are shown in Fig. 19.[113] At low crack-growth rates (~3×10^{-10} to 5×10^{-7} m/cycle), the measured fatigue-crack growth rates (at a given K_{max}) clearly exceed the predicted rates, whereas at higher growth rates (~5×10^{-7} to 1×10^{-5} m/cycle), the predicted rates are similar to slightly faster. This provides strong evidence that at low growth rates, a true cycle-dependent fatigue mechanism is operating in bone, whereas time-dependent sustained-load mechanisms appear to be more important at higher growth rates, the transition occurring

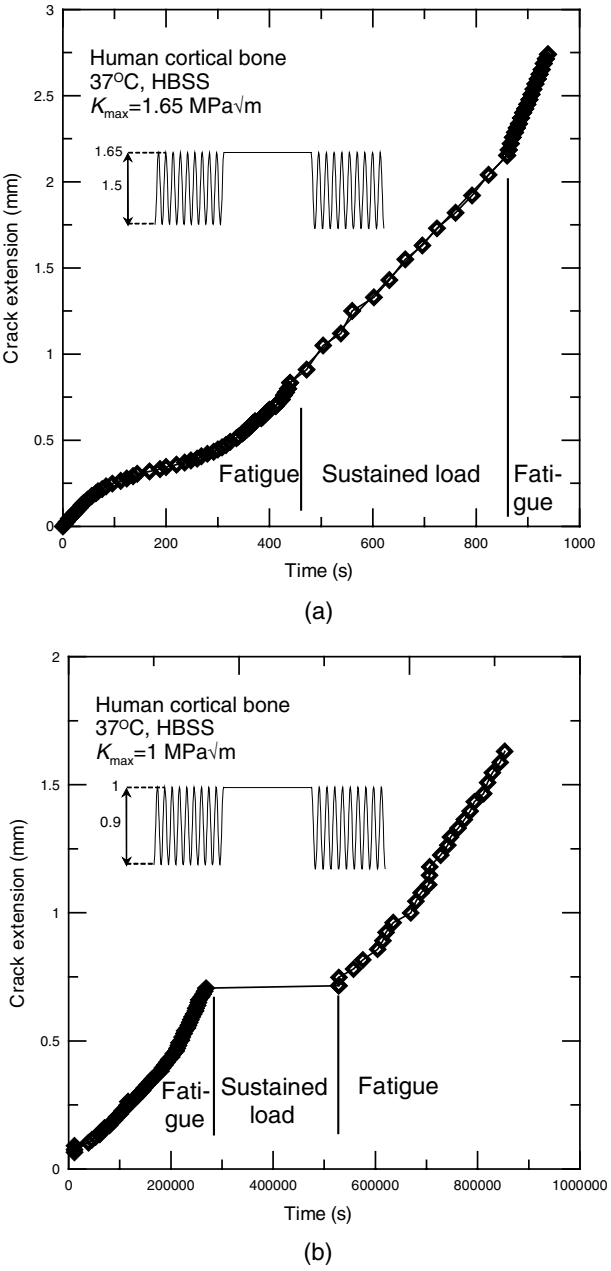

Fig. 18 Results of the 'fatigue-sustained load-fatigue' tests at fixed K_{max} levels, presented as plots of crack extension as a function of time, for (a) $K_{max} = 1.65$ MPa$\sqrt{m}$, (b) $K_{max} = 1$ MPa$\sqrt{m}$ (Nalla *et al.*[113]).

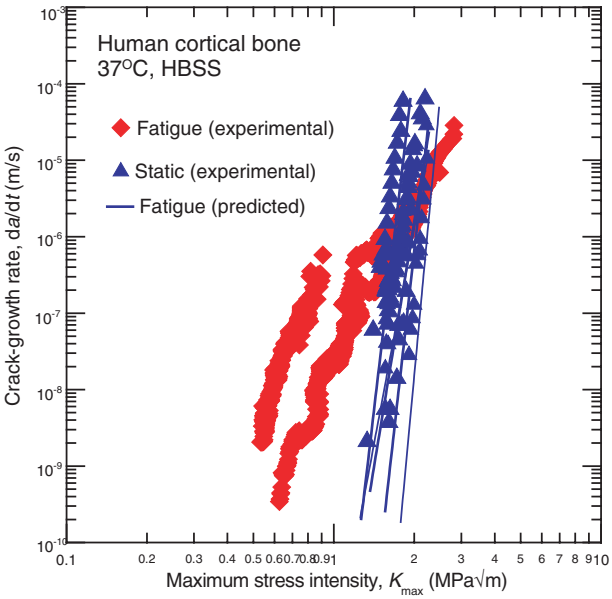

Fig. 19 Comparison of the experimental *in vitro* fatigue-crack growth rate results, expressed as d*a*/d*t* as a function of K_{max}, for human cortical bone with those predicted solely from sustained-load cracking data (Fig. 14), using the Evans and Fuller[114] approach (Eq. 12). Note that experimentally measured growth rates in excess of the Evans–Fuller predictions, as shown for bone below $\sim 10^{-6}$ m/cycle, implies the existence of a "true" cycle-dependent fatigue mechanism in this regime (Nalla *et al.*[113]).

between $\sim 10^{-7}$ and 10^{-6} m/cycle. This transition from static ('creep'-dominated) to cyclic (fatigue-dominated) mechanisms is similar to that suggested by Carter and Caler based on *S/N* data,[123] and subsequently by Taylor.[5] While a specific mechanism for subcritical crack growth under static loading has not been proposed, based on this study,[113] the cyclic mechanism in bone was reasoned to involve crack extension via alternating blunting and re-sharpening of the crack tip (Fig. 20), akin to that seen in ductile materials, such as metals and polymers.[118]

With the availability of the *in vitro* fatigue-crack growth-rate data for cortical bone (Fig. 17), it is now possible to make estimates of the expected fatigue life for cortical bone containing flaws/cracks of specific dimensions. This involves using a fracture-mechanics approach based on the notion that the life comprised the time or number of loading cycles for the largest pre-existing flaw to propagate to catastrophic failure. This is achieved by integrating the Paris crack–growth relationship in Eq. 11 between the limits of the initial flaw size, a_o, and the critical (final) flaw size, a_c, dictated by the fracture toughness (full details are given in Ref. [113]). The number of loading cycles to cause failure, N_f, is thus a strong function of the in-service stress and initial flaw size, and can be expressed (for $m \neq 2$) as

$$N_f = \frac{2}{(m-2)C'}(Q(a/b)\Delta\sigma_{app})^{-m}\pi^{-m/2}\left[a_o^{1-m/2} - a_c^{1-m/2}\right], \quad (14)$$

where $\Delta\sigma_{app}$ is the in-service cyclic stress range, $Q(a/b)$ is a function dependent upon the geometry, flaw size and shape. Figure 21 gives these lifetimes as a function of the initial flaw size and the applied (in-service) stress.

As a specific case, we consider the presence of an initial flaw 100 μm in size. Such flaws have been observed to occur both naturally and as a result of fatigue loading in cortical bone; indeed there are numerous studies that report incipient crack sizes of 50–400 μm (e.g., Refs [4,121,122,128,129]. For physiologically relevant stresses between 5 and 45 MPa,[2] predicted fatigue lifetimes range from over a billion cycles at a maximum stress of 5 MPa to an unrealistically low 3 000 cycles at 45 MPa, highlighting the likely role of bone remodelling/repair and adaptation, particularly at high stresses. Such processes allow for bone to function at loading levels/conditions where the predicted *in vitro* fatigue lifetimes are negligible. Indeed, the role of (fatigue) damage in inducing repair by remodelling by Basic Multicellular Units (BMU's) is well documented (e.g., Refs [2–4]), as is the role of adaptation when bones change their geometry through modelling to adapt to long-term changes in loading patterns (e.g., Refs [1,5]). (Note that modelling is an adaptive process, unlike remodelling which is repair). Any excessive damage that the fatigue loading induces is repaired through remodelling and may be adapted for in the long run.

CONCLUDING REMARKS

Biological materials such as human cortical bone are clearly highly complex structural materials with mechanical properties dictated by their hierarchical microstructure and an ability to both repair themselves and adapt to changing environmental and loading conditions. It is not surprising then that the problem of the fracture and fatigue of bone is equally complex. In this review, we have attempted to convey that an improved understanding has emerged of late as to the nature of the fracture resistance of cortical bone, involving the development of both intrinsic and extrinsic toughening mechanisms. Specifically, the role of crack bridging in providing a primary contribution to the toughening of bone has been

[2]These choices are based on the stresses that are commonly experienced *in vivo*. Peak strains of 350–2100 $\mu\epsilon$ for typical activities have been reported for strain-gauge-based measurements on the long bones (femur) in humans. [5,130–132] A Young's modulus of 12–22 GPa for secondary osteonal compact bone[5] implies that stress levels of ~5–45 MPa would be expected to be physiologically relevant.

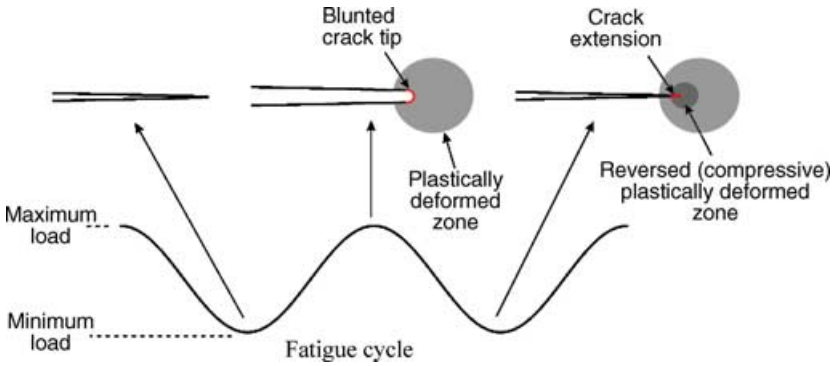

Fig. 20 Schematic illustrating the mechanism of "blunting and resharpening" for fatigue crack growth in cortical bone. The crack is sharp at the beginning of the loading cycle, is blunted at the peak of the loading cycle, and is resharpened (and consequently, extended) after unloading.

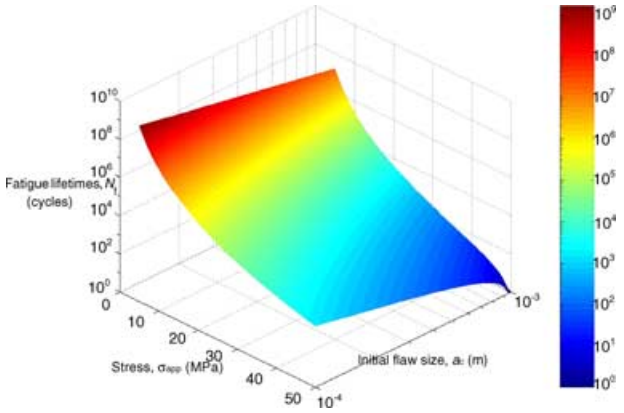

Fig. 21 The predicted fatigue lifetimes, N_f, are shown as a function of the stress, σ_{app}, and the initial flaw size, a_c. Note that a typical bone experiences up to 2×10^6 cycles annually.

highlighted, together with a description of experiments that provide convincing evidence that the onset of fracture in bone is strain-controlled and that subcritical fatigue cracking involves both cycle- and time-dependent mechanisms. However, despite our improved knowledge of how bone fails, a mechanistic understanding of the increased *in vivo* fracture risk associated with factors such as ageing and disease, and how this relates to fracture properties measured *in vitro*, is still relatively limited. The challenge here remains the determination of how specific mechanisms of fracture and fatigue in bone are affected by the microstructure of bone (at nano- to microscales) and how this in turn is affected by biological factors.

A number of other questions remain to be addressed. For example, at the microstructural level, crack bridging has been identified as a potent toughening mechanism although exactly how the uncracked ligaments form is as yet unclear. Similarly, toughening in the transverse orientation by crack deflection has suggested an important role for the cement line; however, an improved understanding of the nature of these interfaces is still needed to fully comprehend their role, particularly in the process of ageing and in conjunction with the use of drugs such as bisphosphonates that affect the remodelling behaviour. Additionally, at smaller size scales, there is little understanding of the effect of deformation at the osteonal level and collagen levels, where transmission electron microscopy can be used to probe incipient deformation and damage. Finally, with respect to fatigue failures, there is still a paucity of relevant crack-growth data for both macro-sized and microcracks under both sustained and cyclic loading. Data concerning, for example, the effect of crack size, far-field compressive loading and mixed-mode loading, remain to be documented.

It is worth noting here that the vast majority of research on bone fracture has focused on cortical bone, which does raise the question as to how relevant these properties are to trabecular bone, the open-celled structure that forms the bulk of both the vertebral body and the femoral neck. It is known, for instance, that the trabecular bone is lamellar, and is a continuation of the lamellae of the endocortical surfaces of the cortical bone. Moreover, the degree of mineralization is the same in the two types of bone, as are the *local* elastic moduli. Differences do exist though at larger (microstructural) length scales; for example, trabecular bone does not have osteons and remodelling occurs only at the surfaces of the trabeculae in contact with the marrow. If the weak interfaces of the cement lines at the osteon/lamellar boundaries are responsible for crack deflection and formation of uncracked ligaments, as we have suggested in this work, then one might expect the fracture toughness of the trabecular bone to be lower than that of cortical bone. However, it is unlikely that trabecular bone fails by the formation of a single, critically sized crack due to the small size of the individual trabeculae. Therefore, the fracture toughness of trabecular bone is reasoned to have little clinical significance and indeed, to our knowledge, there are no studies in archival literature that have looked to measure it. However, other aspects of the failure of trabecular bone including yielding, damage evolution, effect of fatigue, etc. have been well studied.[74–76]

In conclusion, we believe that the understanding developed from studies of the fracture and fatigue behaviour of bone can greatly aid the diagnosis, prevention and treatment of debilitating conditions such as

osteoporosis, which specifically target the key microstructural aspects that provide the resistance to bone failure. Progress has been made with regard to mechanistic understanding, but the degree of this understanding is still limited. Consequently, we believe that bone fracture will continue to remain an area of intense research for the foreseeable future.

Acknowledgements

This work was supported in part by the National Institutes of Health under Grant No. 5R01 DE015633 (for RKN), and by the Director, Office of Science, Office of Basic Energy Science, Division of Materials Sciences and Engineering of the Department of Energy under Contract No. DE-AC03–76SF00098 (for JJK and ROR).

REFERENCES

1 Jones, H. H., Priest, J. D., Hayes, W. C., Tichenor, C. C. and Nagel, D. A. (1977) Human hypertrophy in response to exercise. *J. Bone Joint Surg. A* **59**, 204–208.
2 Burr, D. B., Martin, R. B., Schaffler, M. and Radin, E. L. (1985) Bone remodeling in response to *in vivo* fatigue microdamage. *J. Biomech.* **18**, 189–200.
3 Mori, S. and Burr, D. B. (1993) Increased intracortical remodeling following fatigue damage. *Bone* **14**, 103–109.
4 Lee, T. C., Staines, A. and Taylor, D. (2002) Bone adaptation to load: Microdamage as a stimulus for bone remodelling. *J. Anat.* **201**, 437–446.
5 Taylor, D. (2003) Failure processes in hard and soft tissues. In: *Comprehensive Structural Integrity: Fracture of Materials from Nano to Macro* (Edited by I. Milne, R. O. Ritchie and B. L. Karihaloo) Vol. 9, pp. 35–96. Elsevier, Oxford, U.K.
6 Hui, S. L., Slemenda, C. W. and Johnston, C. C. (1988) Age and bone mass as predictors of fracture in a prospective study. *J. Clin. Invest.* **81**, 1804–1809.
7 Jennings, A. G. and de Boer, P. (1999) Should we operate on nonagenarians with hip fractures? *Injury* **30**, 169–172.
8 Kiebzak, G. M. (1991) Age-related bone changes. *Exp. Gerontol.* **26**, 171–187.
9 Aspray, T. J., Prentice, A., Cole, T. J., Sawo, Y., Reeve, J. and Francis, R. M. (1996) Low bone mineral content is common but osteoporotic fractures are rare in elderly rural Gambian women. *J. Bone Miner. Res.* **11**, 1019–1025.
10 Heaney, R. (2003) Is the paradigm shifting? *Bone* **33**, 457–465.
11 Riggs, B. L., Melton III L. J. and O'Fallon, W. M. (1996) Drug therapy for vertebral fractures in osteoporosis: Evidence that decreases in bone turnover and increases in bone mass both determine antifracture efficacy. *Bone* **18**, 197S–201S.
12 Iwamoto, J. and Takeda, T. (2003) Stress fractures in athletes: Review of 196 cases. *J. Orthop. Sci.* **8**, 273–278.
13 Burr, D. B. (1997) Bone exercise and stress fractures. *Exerc. Sport Sci. Rev.* **25**, 171–194.
14 Meurman, K. O. and Elfving, S. (1980) Stress fracture in soldiers: A multifocal bone disorder. A comparative radiological and scintigraphic study. *Radiology* **134**, 483–487.
15 An, Y. H. (2000) Mechanical properties of bone. In: *Mechanical Testing of Bone and the Bone-Implant Interface*. pp. 41–63. CRC Press, Boca Raton, Florida, U.S.A.
16 Rho, J. Y., Kuhn-Spearing, L. and Zioupos, P. (1998) Mechanical properties and the hierarchical structure of bone. *Med. Engng Phys.* **20**, 92–102.
17 Weiner, S. and Wagner, H. D. (1998) The material bone: Structure-mechanical function relations. *Ann. Rev. Mater. Sci.* **28**, 271–298.
18 Currey, J. D. (1982) 'Osteons' in biomechanical literature. *J. Biomech.* **15**, 717.
19 Wang, X., Shen, X., Li, X. and Agrawal, C. M. (2002) Age-related changes in the collagen network and toughness of bone. *Bone* **31**, 1–7.
20 Lucksanambool, P., Higgs, W. A. J., Higgs, R. J. E. D. and Swain, M. W. (2001) Fracture toughness of bovine bone: Influence of orientation and storage media. *Biomaterics.* **22**, 3127–3132.
21 Wang, X., Bank, R., Tekoppele, J. and Agrawal, C. (2001) The role of collagen in determining bone mechanical properties. *J. Orthop. Res.* **19**, 1021–1026.
22 Currey, J. D. (1979) Changes in impact energy absorption with age. *J. Biomech.* **12**, 459–469.
23 Currey, J. D., Brear, K. and Zioupos, P. (1996) The effects of aging and changes in mineral content in degrading the toughness of human femora. *J. Biomech.* **29**, 257–260.
24 Zioupos, P. and Currey, J. D. (1998) Changes in the stiffness, strength, and toughness of human cortical bone with age. *Bone* **22**, 57–66.
25 Knott, J. (1976) *Fundamentals of fracture mechanics*. Butterworth & Co. (Publishers) Ltd., London, U.K.
26 Norman, T. L., Nivargikar, S. V. and Burr, D. B. (1996) Resistance to crack growth in human cortical bone is greater in shear than in tension. *J. Biomech.* **29**, 1023–1031.
27 Brown, C. U. and Norman, T. L. (1995) Fracture toughness of human cortical bone from the proximal femur. *Adv. Bioeng.* **31**, 121–122.
28 Yeni, Y. N. and Norman, T. L. (2000) Fracture toughness of human femoral neck: Effect of microstructure, composition, and age. *Bone* **26**, 499–504.
29 Feng, Z., Rho, J., Han, S. and Ziv, I. (2000) Orientation and loading condition dependence of fracture toughness in cortical bone. *Mater. Sci. Engng C* **C11**, 41–46.
30 ASTM E399–90 (2002) In: *Annual Book of ASTM Standards, Vol. 03.01: Metals Mechanical Testing; Elevated and Low-temperature Tests; Metallography*. ASTM, West Conshohocken, Pennsylvania, U.S.A.
31 Currey, J. D. (1998) Mechanical properties of vertebrate hard tissues. *Proc. Instn. Mech. Engrs H* **212**, 399–412.
32 Wright, T. M. and Hayes, W. C. (1977) Fracture mechanics parameters for compact bone—Effects of density and specimen thickness. *J. Biomech.* **10**, 419–430.
33 Behiri, J. C. and Bonfield, W. (1984) Fracture mechanics of bone—The effects of density, specimen thickness, and crack velocity on longitudinal fracture. *J. Biomech.* **17**, 25–34.
34 Norman, T. L., Vashishth, D. and Burr, D. B. (1995) Fracture toughness of human bone under tension. *J. Biomech.* **28**, 309–320.
35 Behiri, J. C. and Bonfield, W. (1989) Orientation dependence of the fracture mechanics of cortical bone. *J. Biomech.* **22**, 863–872.
36 Phelps, J. B., Hubbard, G. B., Wang, X. and Agrawal, C. M. (2000) Microstructural heterogeneity and the fracture toughness of bone. *J. Biomed. Mater. Res.* **51**, 735–471.

37 Nalla, R. K., Kinney, J. H. and Ritchie, R. O. (2003) Mechanistic fracture criteria for the failure of human cortical bone. *Nat. Mater.* **2**, 164–168.
38 Brown, C. U., Yeni, Y. N. and Norman, T. L. (2000) Fracture toughness is dependent on bone location—A study of the femoral neck, femoral shaft, and the tibial shaft. *J. Biomed. Mater. Res.* **49**, 380–389.
39 Yeni, Y. N., Brown, C. U. and Norman, T. L. (1998) Influence of bone composition and apparent density on fracture toughness of the human femur and tibia. *Bone* **22**, 79–84.
40 Yeni, Y. N., Brown, C. U., Wang, Z. and Norman, T. L. (1997) The influence of bone morphology on fracture toughness of the human femur and tibia. *Bone* **21**, 453–459.
41 Seeman, E. (1999) The structural basis of bone fragility in men. *Bone* **25**, 143–147.
42 Moyle, D. D. and Bowden, R. W. (1984) Fracture of human femoral bone. *J. Biomech.* **17**, 203–213.
43 Wang, X. D., Masilamani, N. S., Mabrey, J. D., Alder, M. E. and Agrawal, C. M. (1998) Changes in the fracture toughness of bone may not be reflected by its mineral density, porosity, and tensile properties. *Bone* **23**, 67–72.
44 Corondan, G. and Haworth, W. L. (1986) A fractographic study of human long bone. *J. Biomech.* **19**, 207–218.
45 Norman, T. L. and Wang, Z. (1997) Microdamage of human cortical bone: Incidence and morphology in long bones. *Bone* **20**, 375–379.
46 Burr, D. B., Schaffler, M. B. and Frederickson, R. G. (1988) Composition of the cement line and its possible mechanical role as a local interface in compact bone. *J. Biomech.* **21**, 939–945.
47 Yeni, Y. N. and Norman, T. L. (2000) Calculation of porosity and osteonal cement line effects on the effective fracture toughness of cortical bone in longitudinal crack growth. *J. Biomed. Mater. Res.* **51**, 504–509.
48 Martin, R. B. and Burr, D. B. (1982) A hypothetical mechanism for the stimulation of oteonal remodeling by fatigue damage. *J. Biomech.* **15**, 137–139.
49 Nalla, R. K., Kruzic, J. J., Kinney, J. H. and Ritchie, R. O. (2005) Mechanistic aspects of fracture and R-curve behavior in human cortical bone. *Biomater.* **26**, 217–231.
50 Wang, X., Li, X., Bank, R. A. and Agrawal, C. M. (2002) Effects of collagen unwinding and cleavage on the mechanical integrity of the collagen network in bone. *Calcif. Tissue Int.* **71**, 186–192.
51 Pashley, D. H., Agee, K. A., Carvalho, R. M., Lee, K. W., Tay, F. R. and Callison, T. E. (2003) Effects of water and water-free polar solvents on the tensile properties of demineralized dentin. *Dent. Mater.* **19**, 347–352.
52 Burstein, A., Reilly, D. and Martens, M. (1976) Aging of bone tissue mechanical properties. *J. Bone Joint Surg. A* **58**, 82–86.
53 Zioupos, P., Currey, J. D. and Hamer, A. J. (1999) The role of collagen in the declining mechanical properties of aging human cortical bone. *J. Biomed. Mater. Res.* **2**, 108–116.
54 Bonfield, W., Behiri, J. C. and Charalamides, C. (1985) Orientation and the age-related dependence of the fracture toughness of cortical bone. In: *Biomechanics: Current Interdisiplinary Research* (Edited by S. M. Perren and E. Schneider). Martinum Nijhoff Publishers, Dordrecht, Netherlands.
55 Wang, X. D., Masilamani, N. S., Mabrey, J. D., Alder, M. E. and Agrawal, C. M. (1998) Changes in the fracture toughness of bone may not be reflected in its mineral density, porosity, and tensile properties. *Bone* **23**, 67–72.
56 Akkus, O., Adar, F. and Schaffler, M. B. (2004) Age-related changes in physicochemical properties of mineral crystals are related to impaired mechanical function of cortical bone. *Bone* **34**, 443–453.
57 Thompson, D. D. (1980) Age changes in bone mineralization, cortical thickness, and haversian canal area. *Calcif Tissue Int.* **31**, 5–11.
58 Grynpas, M. D. and Holmyard, D. (1988) Changes in quality of bone mineral on aging and in disease. *Scan Microsc.* **2**, 1045–1054.
59 Simmons, E. D. J., Pritzker, K. P. and Grynpas, M. D. (1991) Age-related changes in the human femoral cortex. *J. Orthop. Res.* **9**, 155–167.
60 Lawn, B. R. (1983) Physics of fracture. *J. Am. Ceramic Soc.* **66**, 83.
61 Ritchie, R. O. (1988) Mechanisms of fatigue crack propagation in metals, ceramics and composites: Role of crack-tip shielding. *Mater. Sci. Engng* **103**, 15–28.
62 Ritchie, R. O. (1999) Mechanisms of fatigue-crack propagation in ductile and brittle solids. *Int. J. Fract.* **100**, 55–83.
63 Evans, A. G. (1990) Perspective on the development of high toughness ceramics. *J Am Ceramic Soc.* **73**, 187–206.
64 Vashishth, D., Behiri, J. C. and Bonfield, W. (1997) Crack growth resistance in cortical bone: Concept of microcrack toughening. *J. Biomech.* **30**, 763–769.
65 Vashishth, D., Tanner, K. E. and Bonfield, W. (2000) Contribution, development and morphology of microcracking in cortical bone during crack propagation. *J Biomech.* **33**, 1169–1174.
66 Malik, C. L., Stover, S. M., Martin, R. B. and Gibeling, J. C. (2003) Equine cortical bone exhibits rising R-curve fracture mechanics. *J. Biomech.* **36**, 191–198.
67 Pezzotti, G. and Sakakura, S. (2003) Study of the toughening mechanisms in bone and biomimetic hydroxyapatite materials using Raman microprobe spectroscopy. *J. Biomed. Mater. Res. A.* **65**, 229–236.
68 Vashishth, D., Tanner, K. E. and Bonfield, W. (2003) Experimental validation of a microcracking-based toughening mechanism for cortical bone. *J. Biomech.* **36**, 121–124.
69 Vashishth, D. (2004) Rising crack-growth-resistance behavior in cortical bone: Implication for toughness measurements. *J. Biomech.* **37**, 943–946.
70 Nalla, R. K., Kruzic, J. J. and Ritchie, R. O. (2004) On the origin of the toughness of mineralized tissue: Microcracking or crack bridging? *Bone* **34**, 790–798.
71 Nalla, R. K., Kruzic, J. J., Kinney, J. H. and Ritchie, R. O. (2004) Effect of aging on the toughness of human cortical bone: Evaluation by R-curves. *Bone* **35**, 1240–1246
72 Wu, P. C. and Vashishth, D. (2002) Age related changes in cortical bone toughness. In: *2nd Joint EMBS/BMES Conference*. IEEE, Houston, Texas, U.S.A., pp. 425–426
73 Currey, J. D., Brear, K. and Zioupos, P. (1996) The effects of ageing and changes in mineral content in degrading the toughness of human femora. *J. Biomech.* **29**, 257–260.
74 Keaveny, T. M., Wachtel, E. F., Ford, C. M. and Hayes, W. C. (1994) Differences between the tensile and compressive strengths of bovine tibial trabecular bone depend on modulus. *J. Biomech.* **27**, 1137–46.

75 Ford, C. M. and Keaveny, T. M. (1996) The dependence of shear failure properties of trabecular bone on apparent density and trabecular orientation. *J. Biomech.* **29**, 1309–1317.
76 Yeh, O. C. and Keaveny, T. M. (2001) Relative roles of microdamage and microfracture in the mechanical behavior of trabecular bone. *J. Orthop. Res.* **19**, 1001–1007.
77 Evans, A. G. and Faber, K. T. (1984) Crack-growth resistance of microcracking brittle materials. *J. Am. Ceramic Soc.* **67**, 255–260.
78 Hutchinson, J. W. (1987) Crack tip shielding by micro-cracking in brittle solids. *Acta Metallurgica* **35**, 1605–1619.
79 Yeni, Y. N. and Fyhrie, D. P. (2002) Fatigue damage-fracture mechanics interaction in cortical bone. *Bone* **30**, 509–514.
80 Sigl, L. S. (1996) Microcrack toughening in brittle materials containing weak and strong interfaces. *Acta Materialia* **44**, 3599–3609.
81 Yeni, Y. N. and Fyhrie, D. P. (2003) A rate-dependent microcrack-bridging model that can explain the strain rate dependency of cortical bone apparent yield strength. *J. Biomech.* **36**, 1343–1353.
82 Bilby, B. A., Cardew, G. E. and Howard, I. C. (1977) Stress intensity factors at the tips of kinked and forked cracks. In: *Fracture 1977* (Edited byD. M. R. Taplin). Pergamon Press, Oxford, U.K. pp. 197–200.
83 Cotterell, B. and Rice, J. R. (1980) Slightly curved or kinked cracks. *Int. J. Fract.* **16**, 155–169.
84 Nalla, R. K., Stolken, J. S., Kinney, J. H. and Ritchie, R. O. (2005) On micro-mechanisms of in vitro fracture and toughening in human cortical bone. *J. Biomech.* **38**, in press.
85 Shang, J. K. and Ritchie, R. O. (1989) Crack bridging by uncracked ligaments during fatigue-crack growth in SiC-reinforced aluminum-alloy composites. *Metall. Trans. A.* **20**, 897–908.
86 Evans, A. G. and McMeeking, R. M. (1986) On the toughening of ceramics by strong reinforcements. *Acta Metallurgica* **34**, 2435–2441.
87 Evans, A. G. and Faber, K. T. (1984) Crack-growth resistance of microcracking brittle materials. *J. Am. Ceramic Soc.* **67**, 255–260.
88 Sigl, L. S. (1996) Microcrack toughening in brittle materials containing weak and strong interfaces. *Acta Metallurgica* **44**, 3599–3609.
89 Wang, X., Li, X., Bank, R. A. and Agrawal, C. M. (2002) Effect of collagen unwinding and cleavage on the mechanical integrity of the collagen network in bone. *Calcif. Tissue Int.* **71**, 186–192.
90 Evans, F. G. and Lebow, M. (1957) Strength of human compact bone under repetitive loading. *J. Appl. Physiol.* **10**, 127–130.
91 Swanson, S. A., Freeman, M. A. and Day, W. H. (1971) The fatigue properties of human cortical bone. *Med. Biol. Engng* **9**, 23–32.
92 Carter, D. R. and Hayes, W. C. (1976) Fatigue life of compact bone—I. Effects of stress amplitude, temperature and density. *J. Biomech.* **9**, 27–34.
93 Lafferty, J. F. and Raju, P. V. V. (1979) The effect of stress frequency on the fatigue strength of cortical bone. *J. Biomech. Engng* **101**, 112–113.
94 Carter, D. R. and Caler, W. E. (1983) Cycle-dependent and time-dependent bone fracture with repeated loading. *J. Biomech. Engng* **105**, 166–170.
95 Caler, W. E. and Carter, D. R. (1989) Bone creep-fatigue damage accumulation. *J. Biomech.* **22**, 625–635.
96 Schaffler, M. B., Radin, E. L. and Burr, D. B. (1989) Mechanical and morphological effects of strain rate on fatigue of compact bone. *Bone* **10**, 207–214.
97 Boyce, T. M., Fyhrie, D. P., Brodie, F. R. and Schaffler, M. B. (1996) Residual mechanical properties of human cortical bone following fatigue loading. In: *20th Annual Meeting of the American Society of Biomechanics*. American Sociecty of Biomechanics, Atlanta, Georgia, U.S.A.
98 Pattin, C. A., Caler, W. E. and Carter, D. R. (1996) Cyclic mechanical property degradation during fatigue loading of cortical bone. *J. Biomech.* **29**, 69–79.
99 Zioupos, P., Wang, X. T. and Currey, J. D. (1996) The accumulation of fatigue microdamage in human cortical bone of two different ages *in vitro*. *Clin. Biomech.* **11**, 365–375
100 Zioupos, P., Wang, X. T. and Currey, J. D. (1996) Experimental and theoretical quantification of the development of damage in fatigue tests of bone and antler. *J. Biomech.* **29**, 989–1002.
101 Martin, R. B., Gibson, V. A., Stover, S. M., Gibeling, J. C. and Griffin, L. V. (1997) Residual strength of equine bone is not reduced by intense fatigue loading: Implications for stress fracture. *J. Biomech.* **30**, 109–114.
102 Taylor, D. (1998) Microcrack growth parameters for compact bone deduced from stiffness variations. *J. Biomech.* **31**, 587–592.
103 Griffin, L. V., Gibeling, J. C., Martin, R. B., Gibson, V. A. and Stover, S. M. (1999) The effects of testing methods on the flexural fatigue life of human cortical bone. *J. Biomech.* **32**, 105–109.
104 Akkus, O. and Rimnac, C. M. (2001) Cortical bone tissue resists fatigue fracture by deceleration and arrest of microcrack growth. *J. Biomech.* **34**, 757–764.
105 Gibeling, J. C., Shelton, D. R. and Malik, C. L. (2001) Application of fracture mechanics to the study of crack propagation in bone. In: *Structural Biomaterials for the 21st Century*. (Edited by H. Rack, D. Lesuer and E. Taleff), TMS, Warrendale, Pennsylvania, U.S.A., pp. 239–254.
106 Vashishth, D., Tanner, K. E. and Bonfield, W. (2001) Fatigue of cortical bone under combined axial-torsional loading. *J. Orthop. Res.* **19**, 414–420.
107 Zioupos, P., Currey, J. D. and Casinos, A. (2001) Tensile fatigue in bone: Are cycles-, or time to failure, or both, important?. *J. Theor. Biol.* **210**, 389–399.
108 Fleck, C. and Eifler, D. (2003) Deformation behaviour and damage accumulation of cortical bone specimens from the equine tibia under cyclic loading. *J. Biomech.* **36**, 179–189.
109 Hiller, L. P., Stover, S. M., Gibson, V. A., Gibeling, J. C., Prater, C. S., Hazelwood, S. J., Yeh, O. C. and Martin, R. B. (2003) Osteon pullout in the equine third metacarpal bone: Effects of ex vivo fatigue. *J. Orthop. Res.* **21**, 481–488.
110 Martin, R. B. (2003) Fatigue damage, remodeling, and the minimization of skeletal weight. *J. Theor. Biol.* **220**, 271–276.
111 O'Brien, F. J., Taylor, D. and Lee, T. C. (2003) Microcrack accumulation at different intervals during fatigue testing of compact bone. *J. Biomech.* **36**, 973–980.
112 Taylor, D., O'Reilly, P., Vallet, L. and Lee, T. C. (2003) The fatigue strength of compact bone in torsion. *J. Biomech.* **36**, 1103–1109.

113 Nalla, R. K., Kruzic, J. J., Kinney, J. H. and Ritchie, R. O. (2005)Aspects of in vitro fatigue in human cortical bone: Time- and cycle-dependent crack growth. *Biomaterials* **26**, 2183–2195
114 Evans, A. G. and Fuller, E. R. (1974) Crack propagation in ceramic materials under cyclic loading conditions. *Metall. Trans. A* **5**, 27–33.
115 Bonfield, W., Grynpas, M. D. and Young, R. J. (1978) Crack velocity and the fracture of bone. *J. Biomech.* **11**, 473–479.
116 Behiri, J. C. and Bonfield, W. (1980) Crack velocity dependence of longitudinal fracture in bone. *J. Mater. Sci.* **15**, 1841–1849.
117 Caler, W. E. and Carter, D. R. (1989) Bone-creep fatigue damage accumulation. *J. Biomech.* **22**, 625–635.
118 Suresh, S. (1998) *Fatigue of materials*. 2nd edn. Cambridge University Press, Cambridge, U.K.
119 Frost, H. M. (1960) Presence of microscopic cracks *in vivo* in bone. *Henry Ford Hospital Med. Bull.* **8**, 25–35.
120 Lee, T. C., Myers, E. R. and Hayes, W. C. (1998) Fluorescence-aided detection of microdamage in compact bone. *J. Anat.* **193**, 179–184.
121 Lee, T. C., Arthur, T. L., Gibson, L. J. and Hayes, W. C. (2000) Sequential labelling of microdamage in bone using chelating agents. *J. Orthop. Res.* **18**, 322–325.
122 Lee, T. C., Mohsin, S., Taylor, D., Parkesh, R., Gunnlaugsson, T., O'Brien, F. J., Giehl, M. and Gowin, W. (2003) Detecting microdamage in bone. *J. Anat.* **203**, 161–172.
123 Carter, D. R. and Caler, W. E. (1985) A cumulative damage model for bone fracture. *J. Orthop. Res.* **3**, 84–90.
124 Rimnac, C. M., Petko, A. A., Santners, T. J. and Wright, T. M. (1993) The effect of temperature, stress and microstructure on the creep of compact bovine bone. *J. Biomech.* **26**, 219–228.
125 Wright, T. M. and Hayes, W. C. (1976) The fracture mechanics of fatigue crack propagation in compact bone. *Biomed. Mater. Res. Symn. (J. Biomed. Mater. Res.)* **7**, 637–648.
126 Paris, P. C., Gomez, M. P. and Anderson, W. P. (1961) A rational analytic theory of fatigue. *Trend Engng* **13**, 9–14.
127 Asoo, B., McNaney, J. M., Mitamura, Y. and Ritchie, R. O. (2000) Cyclic fatigue-crack propagation in sapphire in air and simulated physiological environments. *J. Biomed. Mater. Res.* **52**, 488–491.
128 Burr, D. B. and Stafford, T. (1990) Validity of the bulk-staining technique to separate artifactual from in vivo bone microdamage. *Clin. Orthop.* **260**, 305–308.
129 O'Brien, F. J., Taylor, D., Dickson, G. R. and Lee, T. C. (2000) Visualisation of three-dimensional microcracks in compact bone. *J. Anat.* **197**, 413–420.
130 Burr, D. B., Milgrom, C., Fyhrie, D., Forwood, M., Nyska, M., Finestone, A., Hoshaw, S., Saiag, E. and Simkin, A. (1996) *In vivo* measurement of human tibial strains during vigorous activity. *Bone* **18**, 405–410.
131 Hillam, R. A. (1996) Ph.D. Thesis. *Response of bone to mechanical load and alterations in circulating hormones*. University of Bristol, Bristol, U.K.
132 Currey, J. D. (2003) How well are bones designed to resist fracture?. *J. Bone Mineral Res.* **18**, 591–598.
133 Robertson, D. M., Robertson, D. and Barrett, C. R. (1978) Fracture toughness, critical crack length and plastic zone size in bone. *J. Biomech.* **11**, 359–364.